UC Irvine
UC Irvine Electronic Theses and Dissertations

Title

Development of an Optogenetic Platform for the Study of Neural Network Activity

Permalink

https://escholarship.org/uc/item/0zc7q4dh

Author

Shim, Seohyun

Publication Date

2019

Peer reviewed|Thesis/dissertation

UNIVERSITY OF CALIFORNIA,
IRVINE

Development of an Optogenetic Platform for the Study of Neural Network Activity

THESIS

submitted in partial satisfaction of the requirements
for the degree of

MASTER OF SCIENCE

in Biomedical Engineering

by

Seohyun Shim

Thesis Committee:
Professor William C. Tang, Chair
Professor Bernard Choi
Professor Daryl Preece

2019

TABLE OF CONTENTS

LIST OF FIGURES

LIST OF TABLES

ACKNOWLEDGMENTS

ABSTRACT OF THE THESIS

Development of an Optogenetic Platform for the Study of Neural Network Activity

By

Seohyun Shim

Master of Science in Biomedical Engineering

University of California, Irvine, 2019

Professor William C. Tang, Chair

Our brain is made up of multiple levels of network activities that allow an individual to perceive, think, and react to the outside environment. These neuronal networks connect different regions of the brain and often activate synchronously to perform a complex mental activity such as memory formation. Despite such critical nature of the neural network, the fundamental understanding of how these mechanisms are not thoroughly understood. Multielectrode array (MEA) is one of the widely used methods for observing the in vitro neural network activity due to its ability to capture signals from multiple neurons at once. However, it has limited functionality for observing signal propagation from a specific group of stimulated neurons. Electrical stimuli that are given by the MEA are prone to crosstalk and is likely to introduce electrical artifact to the data. Using light to stimulate genetically modified neuron has shown a promising result in terms of spatial resolution as a light signal is relatively free from introducing an electric artifact that compromises the resolution. It also allows us to stimulate a specific group of cells in the same culture by modifying them to respond to a different wavelength. In this light, a device was conceived, designed, constructed, and initially tested that incorporated digital light processing (DLP) projector to MEA to combine the advantages of two different methods; i.e., stimulate neurons with high resolution and acquire data from multiple target sites at once. DLP projector utilizes Light Emitting Diodes (LED) and digital micromirror device (DMD) that can form specific patterns to

deliver light to multiple regions simultaneously. The device propagate light reflected off of the DMD towards the cultured neurons, and the induced electrical signal are acquired via electrodes. As this device was designed to have better spatial resolution than systems that only use MEA and be able to induce stimulation on multiple neurons, it allows closer replication of neuron interaction in the brain and provides a deeper understanding of their function.

This thesis has been organized as follow:

Chapter 1 would provide background information by introducing neural network, highlight the neurodegenerative disease, and mention commonly used electrophysiological recording, including intracellular and extracellular methods. Chapter 1 also provide information on the evolution of optical technology in biological studies, development of optogenetics, and what makes it appealing as well as various methods by which light used in optogenetics can be delivered. Chapter 2 goes over the general design, building, and validation of the device as well as the experimental procedure that should be followed to conduct the experiment. Chapter 3 elaborates on the final design of the device as well as results of the light delivery validation and synchronization of the device between the projector and data acquisition device. Finally, Chapter 4 discusses the experiments that should be done to validate the device further as well as the limitation of the current design and the plan for animal testing. After that, it concludes the thesis by mentioning the future outlook on how the device could be implemented in a neural network study and what other question it could help answer.

Chapter 1

Introduction

1.1 Neural Networks

The brain is one of the most critical organs in any living thing. Not only is it a vital organ for survival, but it also allows an organism to perform complex mental functions such as cognition, emotion, and learning. Much of the brain's structure consists of multiple layers of networks that can be as small as an interaction between two protein molecules to as large as one end of the brain communicating to the other end. Due to its multiscale nature, the angle at which we approach the brain activity can also greatly vary in both spatial and temporal scope [1].

The neural circuit has become one of the most researched areas as it acts as the foundation of brain function as it bridges the gap between the molecular level interaction to behaviors of the organism. It has been shown that the interaction between multiple neural circuits induces complex functions such as memory formation by integrating multiple kinds of information, including past experience and current sensory stimuli [2, 3]. It is also notable that the neural circuit is conserved over different animals, including invertebrates
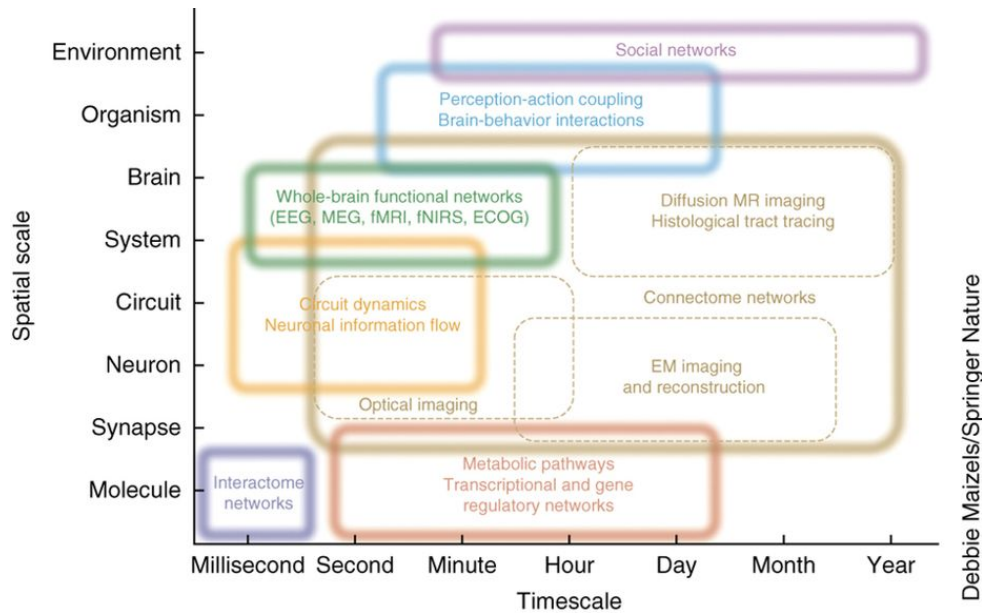
Figure 1.1: Different range of studying brain network (taken from Bassett et al. 2017 [1]).

and vertebrates [4]. This similarity is advantageous as this implies that by understanding the neural circuit and the biomarker associated with the circuit in a model organism, the similar biomarker is likely to be found in human. These factors imply that one of the critical factors in understanding the brain is in knowing more about the neural circuits and their mechanism.

It is a widely accepted fact that the hippocampus plays a crucial role in long-memory formation and retrieval. However, the exact staged encoding mechanism with which it performs such a complex task is not well understood. The association between the hippocampus and spatial memory is relatively well documented, while its association with non-spatial memory such as object recognition still provides conflicting results [5]. Most of the results are obtained either from a behavioral study of a model organism such as mice with differently sized or damaged hippocampus and its subregions [6]. In other words, not enough research is being conducted on the neural circuit level. This lack of coverage may be attributed to the fact that the hippocampus located deep inside the brain and thus is tough to stimulate and gain signal in vivo with high spatial resolution. One of the ways to circumvent this issue is

to use in vitro hippocampal neuron culture to study its circuit. Indeed there was a previous study done on hippocampus neuron cultured on electrode array to understand trisynaptic loop that involves dentate gyrus (DG), cornu ammonis regions 1 and 3 (CA1 and CA3), and entorhinal cortex (EC) [7]. This supports the notion that in vitro neuron study can be an excellent tool to gain an understanding of hippocampal neural circuit that is difficult to control in vivo.

Recently Eytan and Marom showed that "early-to-fire" cells were present in neural circuits that trigger slightly before the others, influencing the activity of other neurons [8]. These neurons are sometimes called "leader neurons" and are assumed to have a more substantial role in forming networks and communicating within neural circuits due to it being connected to more neurons compared to the other. Because it has the potential to play an essential part in communication between the neural circuits, it is worth looking into its role in communication, especially between hippocampal subregions. Observing the characteristics and function of leader neurons are expected to provide new insight into the fundamental mechanism of memory formation and a potential biomarker for diseases associated with memory degradation.

1.2   Neurodegenerative Disease

Neurodegenerative disease is any disease that causes the neurons and by extent brain function to deteriorate over time, which includes Parkinson's, Huntington's, and Alzheimer's diseases (AD). According to the National Institute of Environmental Health Sciences, more than 5.5 million Americans are currently suffering from neurodegenerative disease. Because one of the most significant risk factors for these diseases is age, the number of incidences is expected to rise with the increase of senior population [9]. According to a report produced by the US Census Bureau, the number of people older than 65 represents 8.5 percent of the
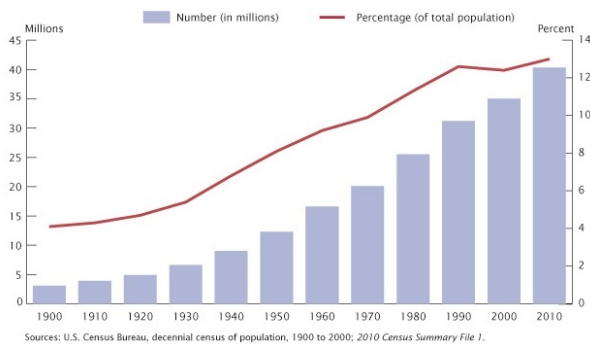
Figure 1.2: Population of 65 years and older by size and percent of total US population (taken from 2010 Census Summary File from US Census Bureau [9]).
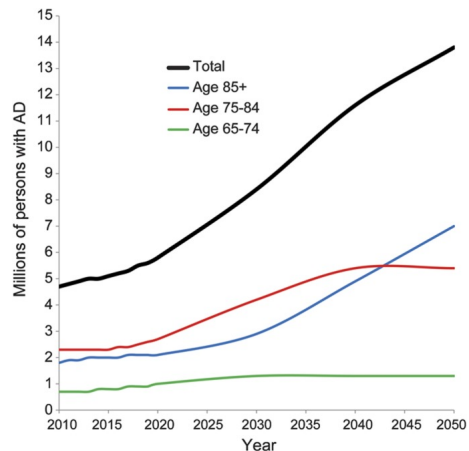
Figure 1.3: Projected increase of Alzheimer's patients (taken from Herbert et al., 2010 [10]).

world population and that percentage is predicted to increase to nearly 17 percent by 2050 (Fig. 1.2). Therefore if this issue is not addressed soon, the number of patients with the neurodegenerative disease could rise to as many as 12 million in 30 years. Thus, the drive to finding the cure for these diseases has been very strong for the last several decades [10].

AD is one of the most common neurodegenerative diseases. According to a statistic provided by Alzheimers' Association, AD affected about 5 million Americans in 2018, and the number of patients is predicted to increase by two folds in the next decade (Fig. 1.3). AD is the 6th leading cause of death in the US but is the only one that does not have a treatment that can slow, stop, or completely cure the condition. In addition to causing suffering on the patient and their family, AD weighs heavily on the health care system and the federal budget. US government had spent an estimated $200 billion in AD patients, and the average Medicare cost for those with AD and other types of dementia is three times higher than people without those conditions. This increased cost is mainly attributed to the co-morbidity that comes with AD. For example, AD patients with diabetes need to spend more money to manage their disease than a patient who only has diabetes [11].

Despite such importance in addressing AD, the development of the cure has not

been fruitful even with over 200 clinical trials during the last two decades [12, 13]. Current drug discovery focuses mainly on the neuropathological features based on amyloidogenic hypothesis, i.e., the assumption that the amyloid beta ($A\beta$) peptide causes plaque buildup in the brain which leads to the neuronal death and cognitive impairment [14]. Another way that is used to modify the disease is to stop the degradation of tau protein, which maintains the structure of the neuron. By preventing tau protein from collapsing, neuronal death caused by the disease could be stopped from propagating. There are also other forms of drugs that are currently in the market such as acetylcholinesterase inhibitor which alleviate symptom associated with lack of acetylcholine, or N-methyl d-aspartate receptor antagonists that removes the excess glutamate produced when brain cells are damaged thereby preventing further damage in healthy brain cells [15, 16]. However, these drugs cannot cure the disease itself, nor can they reverse the damage already done on the brain. To develop a treatment that works on the fundamental level, it is essential to understand the biological pathway and find valid biomarker.

Hippocampus is one of the most distinct regions that is affected by AD, which leads to the early signs of the disease such as memory loss or confusion [17, 18]. The atrophy of the hippocampus in the early stage of AD has been observed via non-invasive imaging techniques such as computed tomography (CT) and magnetic resonance imaging(MRI). Many reported that the volume of hippocampus in AD patients reduces by 15-30% compared to the healthy individuals, which imply an association between the hippocampus and the disease (Fig. 1.4) [19, 20, 17, 21]. However, hippocampal atrophy lacks specificity and sensitivity for AD, especially at an early stage of mild cognitive impairment as it can also be present in the non-AD form of dementia [22, 23].

Recently, hippocampal subregions were found to react differently in the presence of AD with CA1 showing the most shape alteration and volume reduction. Therefore more attention had been increasingly given to hippocampal subregion for predicting pathological
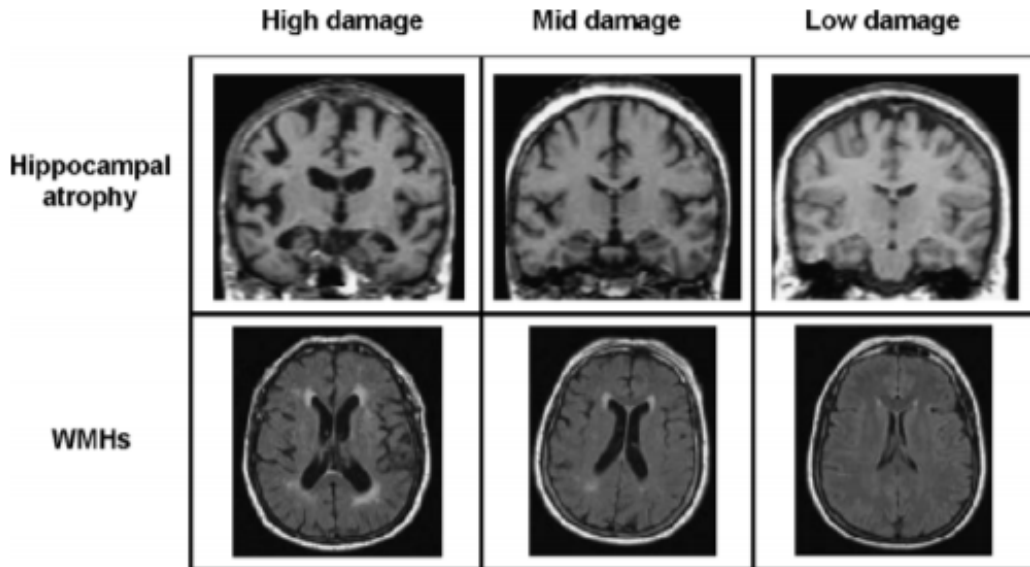
Figure 1.4: Example of hippocampal and white matter atrophy in mild cognitive impairment patients (taken from Moretti et al., 2009 [24]

alteration. The entorhinal cortex (EC), which connects the neocortex to the hippocampus and thus is the gateway for the hippocampus to receive the information flow, was another one that was identified as the core AD marker [25]. It was discovered to show early accumulation of neurofibrillary tangle (NFT), which is one of the hallmarks of AD, and many AD patients were observed to have EC with decreased volume and thickness [26, 27, 28, 29]. However, atrophy in hippocampal subregions is challenging to observe using the traditional imaging method such as MRI because the EC boundaries are often not very clear to see [30]. This difficulty in identifying the exact location of the EC poses as a challenge when attempting to use EC atrophy as a biomarker for AD.

To find out what the fundamental mechanisms of brain functions are and how each can be compromised due to a disease, it is imperative to understand the underlying neural circuits that process those functions. With the development of technology such as optogenetics and calcium imaging, neural activity is now able to be measured to link the neural circuitry to their functions in the brain [31, 32]. Using this technology to find out what goes wrong in the neural circuit in a diseased individual could be very beneficial in identifying

the target for new drug discovery that can cure the disease.

1.3   Electrophysiological Recording

Every eukaryotic cell utilizes selective ion transport across the membrane for survival. Due to the different concentration of a variety of ions such as sodium and potassium, an electrical potential difference occurs between intracellular and extracellular space and causes the electrical current that can be measured [33]. Electrophysiological recording takes advantage of this and observes this current to understand the cell activity. This technique is particularly useful when studying excitable cells such as muscle cells or neurons as they produce current when performing a necessary function such as muscle contraction or nerve conduction. Electrophysiological recording can be performed either in vivo or in vitro with each having its advantage over the other in certain areas.

The advantage of in vivo recording is that it can monitor the neural activity of an organism that is in its natural state. This is crucial for some experiments as not every condition in vivo can be replicated in vitro, thus requires a live animal to conduct the study. Also, in vivo recording allows for observation on the whole body in response to particular stimulus instead of focusing on small specific part [34]. Knowing the overall effect on the body is crucial, especially in pharmaceutical or medical study as it provides insight into what side effects to look out for when targeting specific biomarker to treat a disease. In vivo experiment also enables screening for drugs on the long-term effect on an organism [34, 35]. Despite these advantages, in vivo experiments are very hard to control and often requires in-dept understanding on the mechanism to understand the result correctly.

In vitro study, on the other hand, is much easier to control the environment for the experiment. Due to its relative simplicity, in vitro cultured neurons are often used to gain

more insight into the fundamental mechanism of neural activity and to study the circuit dynamics. While 2D in vitro culture may not necessarily have the same formation as the in vivo tissue, it has been shown in previous studies that the neurons in culture show similar characteristics regarding the formation of networks as in vivo. Especially the fact that hippocampus retains its directionality when cultured in vivo implies that the neural network required for communication between hippocampal subregions and possibly the underlying mechanism of memory formation can be observed in vitro in a controlled environment [7].

Cultured tissue is beneficial in that one animal can produce multiple samples that can be used in multiple experiments. For instance, hippocampal neurons are often cultured by 1,000 cells/mm^2 density. Since the total number of neurons in hippocampus can be as high as 21,000 cells/mm^3, even under the assumption that not all neurons successfully grow in vitro, many samples can be obtained from one brain [36]. Compared to in vivo experiment where one animal is needed per experiment, in vitro method can reduce the number of animals needed to be sacrificed for the experiment.

Due to their usefulness, many methods were developed over the years in the field of electrophysiology for many different purposes in the neural study. Some of the most prominent methods include intracellular recording using sharp or patch electrodes, and extracellular recording with microelectrode array.

1.3.1 Intracellular recording

Intracellular recording measures the change in cellular membrane potential by having one electrode act as a ground while the other electrode records potential from the interior of the cell membrane. Getting access to the interior potential is done either by piercing through the membrane using a sharp electrode or forming a seal with a giga-ohm resistance on the membrane using patch clamp. Although sharp electrode recording is the more traditional
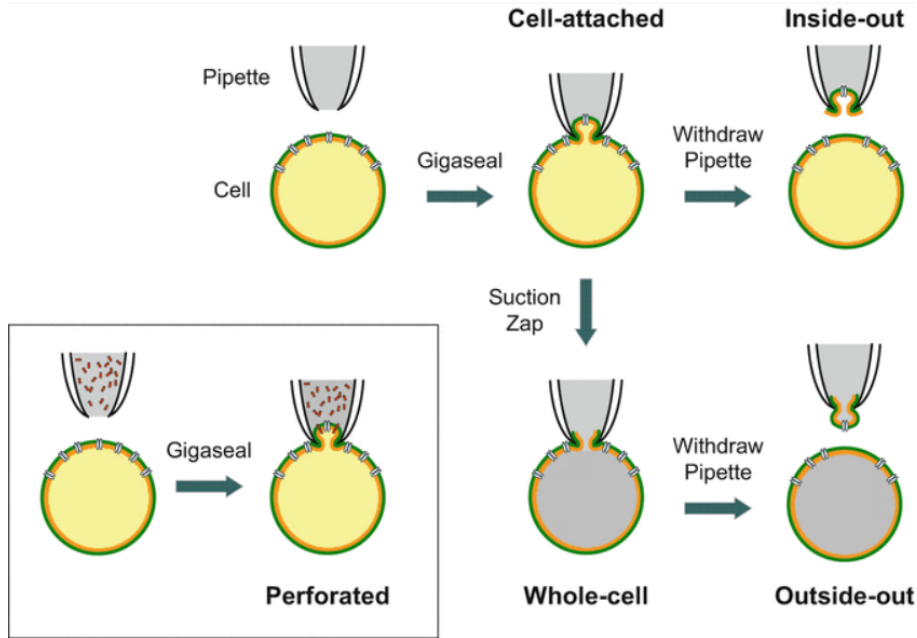
Figure 1.5: Different ways patch clamp can measure membrane potential (taken from Chen et al., [37]).

method of the two, patch clamp has the advantage of not needing to disrupt the cell membrane too much and thus can record the electrical activity of a cell in a more natural state. For this reason, the patch clamp method is currently used very frequently for both in vivo and in vitro electrophysiological recording [38].

The patch clamp method involves a flat, blunt open glass pipette. By being attached to the outer cell membrane via suction, the pipette can act as a microelectrode. This method allows for a recording of the currents through the ion channel on the cell membrane that is sucked into the glass pipette (Fig. 1.5). This method directly measures the current flowing through the cell membrane; therefore, it is very specific and sensitive. Because of this sensitivity, patch clamp is used very often in neural activity recording, especially on studying single neuron dynamics related to behavior [39]. With the help of optogenetics, which can ensure high temporal resolution when stimulating the neurons, the patch clamp proves to be an excellent tool for studying the electrical current flow in single excitable cell [40, 41]. However, using patch clamp is not ideal when trying to study the neural network activity of
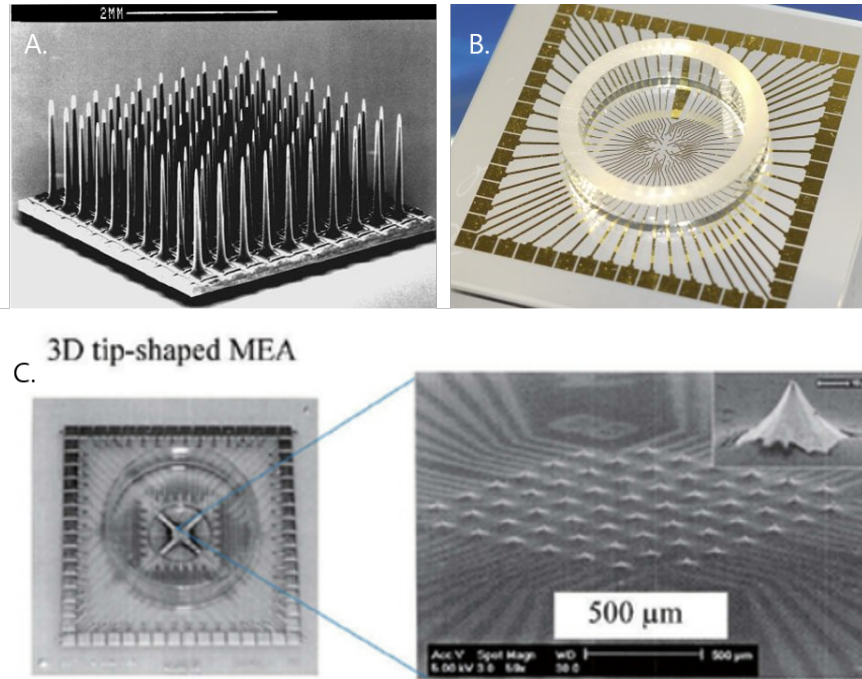
Figure 1.6: Different types of MEAs. A. Utah style array (taken from Kim et al., 2006 [43]) B. Planar electrode array (taken from multichannel system webpage [44]) C. 3D tip-protruding MEA chip (taken from Liu et al., 2012 [45]).

multiple neurons, as it can only record up to 4 neurons at one time. Although some patch clamp devices were made that has up to 20 recording sites with the help of optogenetics, gathering enough data to obtain the overall picture of the neural activity remains a daunting task [42].

1.3.2 Extracellular recording

Extracellular recording measures the change in electrical potential around the extracellular space of a cell when the ion flows through the cell membrane, i.e., local field potential (LFP). It can either measure the potential from a single cell or multiple cells depending on the size of the electrode or purpose of the study.

Multielectrode array (MEA) is often used for this purpose as it can measure multiple

neurons at once depending on how many electrodes are present [46]. This capability allows for an observation on the spontaneous activity or responses from multiple neurons after a stimulus. Thus MEA is often used for drug screening to identify the drug's effect on neural tissue. There are many different kinds of MEA depending on their purpose including the ones with sharp electrodes in vivo recording, a planar electrode for general neural culture, and 3-dimensional(3D) tipped electrodes for piercing through the dead layer of a brain slice to get better activation (Fig. 1.6).

With increased density of electrodes comes lower signal to noise ratio due to electrical signals affecting not only the cells that are placed on the electrode but the neighboring cells as well. This capacitive coupling (i.e., crosstalk) can compromise the spatial resolution as the association between the recorded signals, and the stimulation that was provided gets blurry [47]. Many research is being conducted on addressing this issue by either minimizing the electrode impedance [47], introducing voltage bias [48], or applying an algorithm to remove the effect of crosstalk afterward [49]. Nevertheless, the existence of crosstalk that increases proportional to the density of the electrodes and the intensity of the stimuli still acts as a hindrance to recording neural network activity.

1.4   Optical technology in biological study

1.4.1   Overview of Optical technology

Study of light and its properties has been around since the ancient times [50]. As visual perception is the most used sense for observation, the drive to find ways to see the world better had always been active in human history. With the invention of spectacles in the 14th century, an early form of a telescope was developed in the late 16th century by the Lippershey and the Jassens who were famous spectacle makers. A compound microscope, which is a

reverse telescope, was also developed by the same makers using two lenses [51]. Since then, more microscopes were developed to have lower chromatic and spherical aberration.

While the development of optical system allowed the diffraction limit of light limits the observation of small biological organism, the resolution of the optical system using visible light. i.e., if two objects are closer than $\lambda/2NA$ distance away from each other with λ being the wavelength of light and NA being the numerical aperture(NA) of the objective lens, it is impossible to tell them apart [51]. Even the state-of-the-art highly corrected objective lens has the maximum NA of 1.3-1.6, the highest spatial resolution possible for optical imaging was limited to ~180nm until as recently as 2010 [52]. This limitation posed as a challenge when observing subcellular organelle as it could be as small as 100nm.

In the 1960s, Shimomura et al. discovered a way to extract green fluorescent protein (GFP) from the jellyfish *Aequorea victoria* [53]. What differentiated this protein from other similar bioluminescent proteins was that there were no additional chemical or enzyme needed to activate the light. The gene sequence of this protein was promptly cloned in the 1990s and is used to this day in various studies [54]. GFP was initially used for in vivo gene expression but soon was actively utilized in genetic fusion tag to certain proteins and observing the localization of target protein [55]. Thus, GFP and fluorescence microscopy opened a new door for observing transcriptional pathway and protein interaction.

To enable closer examination of these proteins with GFP, overcoming the limitation of the diffraction barrier was essential. This need led to the development of new optical technology using fluorescence molecules called Photo-Activated Localization Microscopy (PALM) [56]. For this microscope, fluorescent proteins are randomly chosen to be stimulated, and the point spread function of the small subset of cells are acquired from the target site. Then the molecules are photobleached, and another subset is chosen to be activated. By aggregating the data obtained from multiple instances of turning the fluorescent molecules on and off, the actual image can be recreated with much high resolution of up to 10-20nm[56, 57].
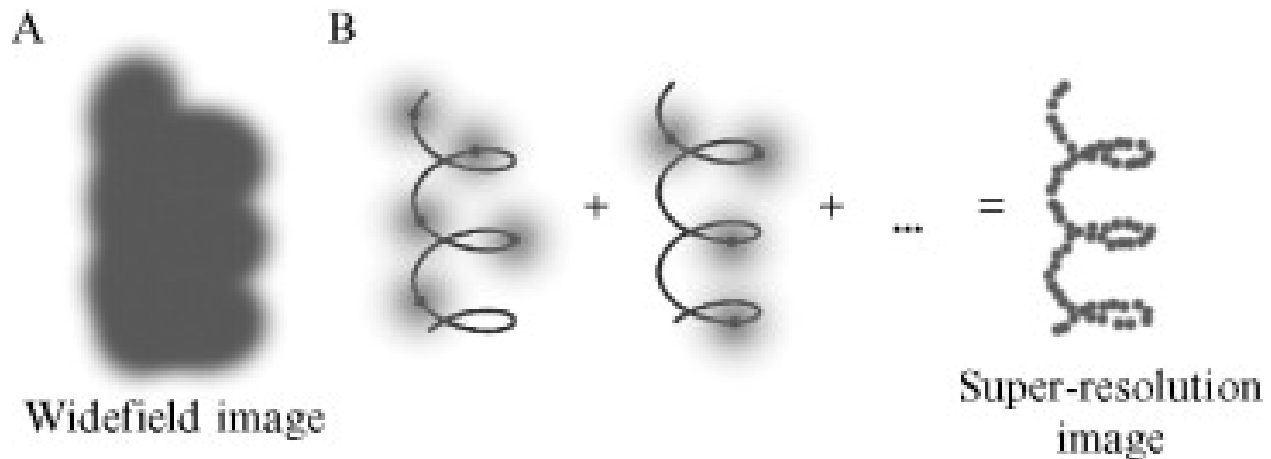
Figure 1.7: Schematic for super-resolution image using PALM (taken from Thompson et al., 2010 [52]).

Although fluorescence gene can be inserted to individual promoters to observe only the specific protein of an organism, this gets little trickier when attempting to examine sample that is not single layered. The fluorescent light from multiple focal planes all lie on top of each other to create a single two-dimensional image that blurs the actual proteins that we were trying to target. To solve this problem, a confocal microscope which enhances the resolution and contrast of the image by focusing on a single point in a specific focal plane is often used. This resolution is achieved by introducing confocal pinhole into the optical system and effectively blocking out the images from other focal planes that are out of focus. Each image can later be used to produce a 3D reconstruction of the sample [58, 59]. Two-photon microscopy (TPM) is another one of the fluorescence microscopes that mainly aim to image the three-dimensional structure of tissue that is thicker than a few hundred micrometers. Instead of using a pinhole to block out the images that were created out of focus, it scans over the focal plane with low-energy photons using the x-y scanner and only detect fluorescence when two photons combine to have enough energy to elicit a response.

From using natural visible light to using a laser to elicit a response, the optical technology has evolved to use light not only something to observe but a tool to better focus on the target while reducing the rest. Recently, more active use of the element emerged as

13
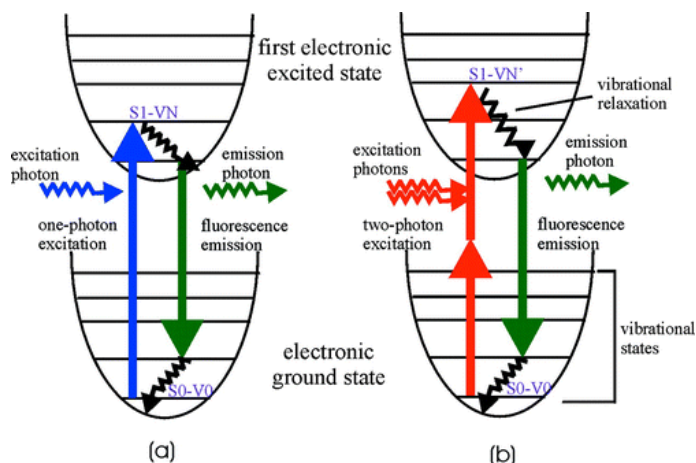
Figure 1.8: Jablonski diagram of (a) one-photon and (b) two-photon excitation (taken from So et al., 2000 [60]).

light is used to intentionally induce activity from the living cells with the same tool used to activate the fluorophores within the microscope [61].

1.4.2   Principle of Optogenetics

Ever since the discovery of bacteriorhodopsin, a retinal protein that acts as light-activated single-component ion pump found in halobacteria that can control the ion flow with within millisecond, optogenetics has become a vital tool for many researchers [62] (Figure 1.10). Optogenetics combines genetic and optical method and provides a way to stimulate and elicit a response from specific cells either in vivo or in vitro. The first protein to be used as an optogenetic tool in the central nervous system was channelrhodopsins that react to blue (460nm) light integrated into hippocampal neuron [63]. In the years that followed, more single-component proteins were found that were capable of being activated in a different wavelength of light. Some of the examples of these microbial opsin gene family are bacteriorhodopsin (BR) which is a light-gated proton pump, halorhodopsin (HR) which is a chloride pump, or channelrhodopsin (ChR) which lets in ion-flux proteins [64]. For neural stimulation, however, ChR with its ability to let cation flow into the cell is ideal as it causes
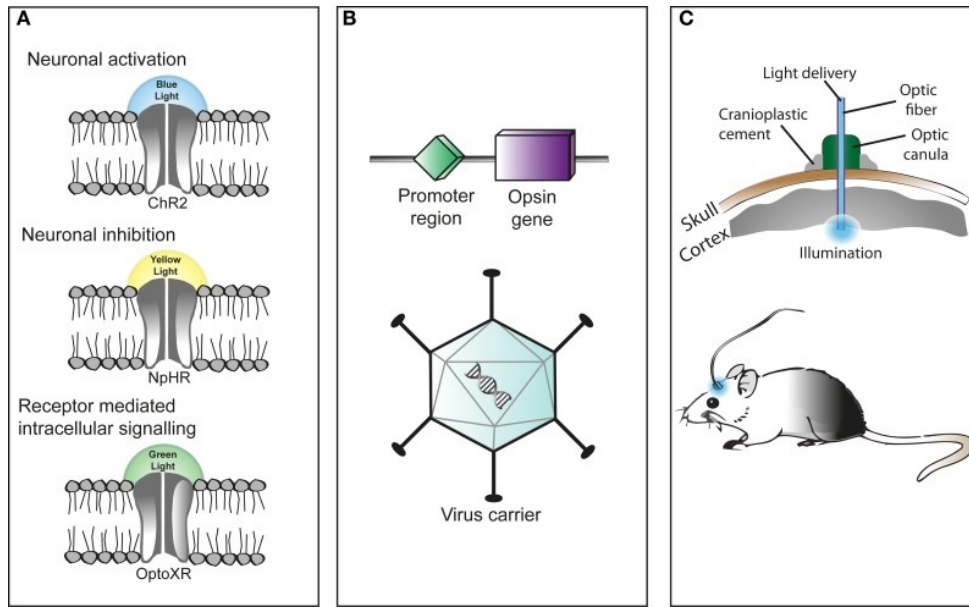
Figure 1.9: Steps for applying optogenetic techniques for in vivo stimulation. A. choose the type of opsin used, B. insert opsin gene via viral carrier, and C. stimulation using light emitting instrument (taken from Pama et al., 2013 [65]).

depolarization of neuron to trigger action potential and induce chain reaction from other connected neurons.

For the cell to react to light, microbial opsin of choice is integrated into the cell membrane by inserting the opsin gene into the target cell. Inserting these genes is done either by breeding transgenic animal or using viral transduction on wildtype animal with adeno-associated virus (AAV) [66]. Viral transduction is more prevalent for in vivo expression process as it provides opsin to a small area of the brain that should be stimulated [67]. It is also beneficial in in vitro settings as it has a relatively high level of expression. However, viral transduction cannot guarantee all the neurons to be infected and can yield an uneven result. Transgenic animal tends to have lower opsin expression level than the viral method but shows a more consistent expression over all neurons. Therefore, if the experiment calls for even expression of opsin, a transgenic animal would be better suited for the purpose than attempting viral transduction [68].

Increase of scientific literature in optogenetics
with the development of relevant techonology
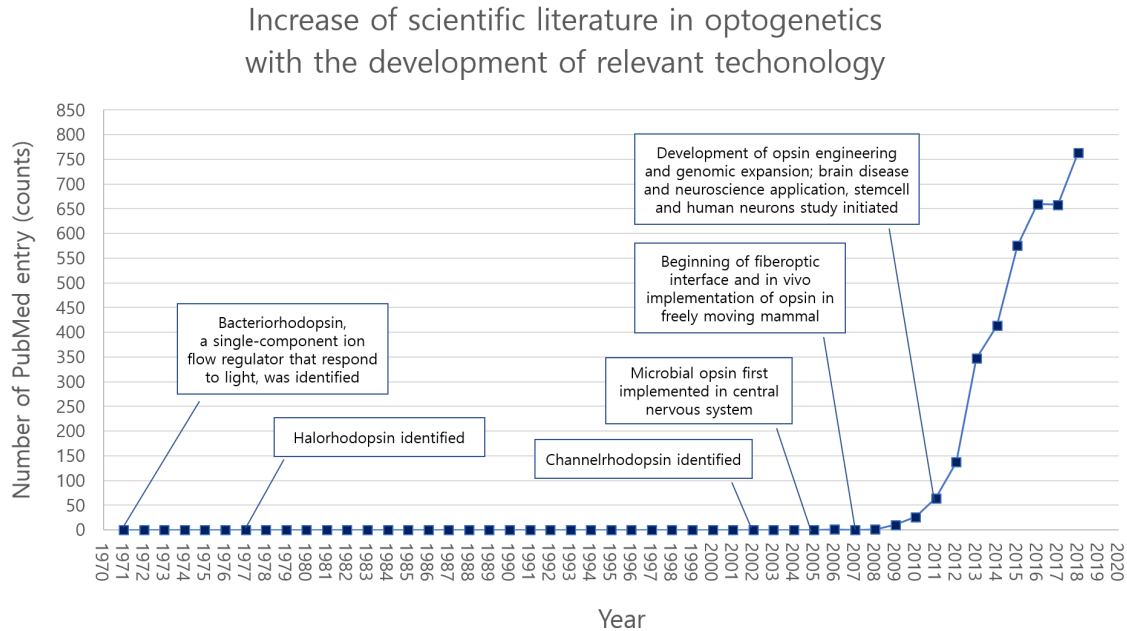
Figure 1.10: Recent increase of 'optogenetic' in scientific literature. Reconstructed from graph taken from Deisseroth et al., 2011 [69].

1.4.3 Advantage of Optogenetcs

Optogenetics has several key advantages that make it appealing. The most prominent one is that once inserted, microbial opsins expressed on the cell membrane respond to light and allow ion flow into the cells in millisecond precision [69]. Before optogenetics was utilized, if researchers wanted to control cellular activity, methods such as genetic modification, pharmacological modulation, or temperature-sensitive mutations were used. These methods either targeted less specific areas or took a long time to activate, which is not ideal for studying neural activity where the result of a stimulus can occur in a relatively short amount of time and can propagate to trigger a wide range of reactions [70]. Therefore, the specificity and speed offered by optogenetics have opened up a new horizon for studying simultaneous input-output interrogation of excitable tissue.

Because optogenetics utilizes light to trigger response and not an electrical signal, it has a relatively low chance of inducing crosstalk. Crosstalk in electrophysiology had been

16
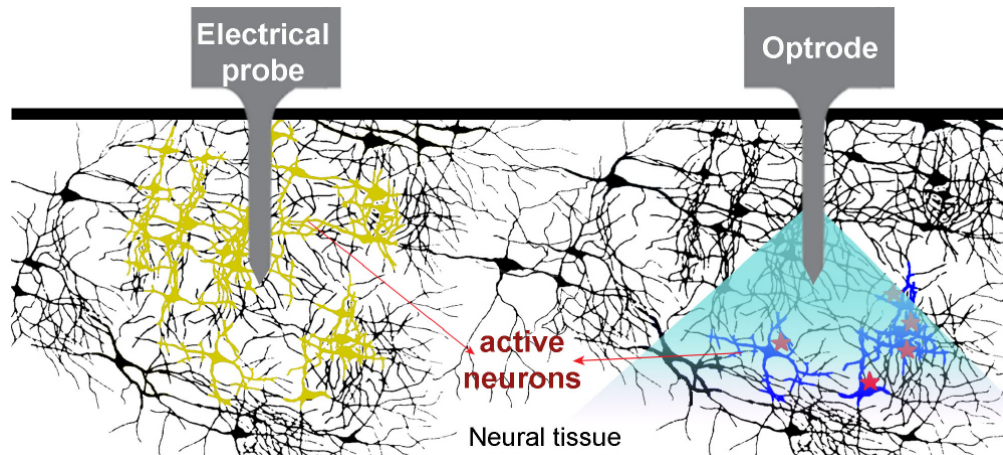
Figure 1.11: Electrical signal versus light signal in vivo. While electrical signal stimulate all the neurons that are around the probe, light signal only stimulate those that are modified (taken from Goncalves et al., 2017 [71]).

a significant issue, especially since many of the extracellular recordings are done with MEA that benefits from having more recording sites. As light stimuli do not travel through the media as much as the electrical stimuli do, it is relatively free from causing crosstalk during the experiment.

1.4.4   Light delivery methods

Network activity within neural circuit often requires stimulation from multiple neurons. Therefore, optogenetic stimulation on multiple target sites is necessary to mimic the function that occurs in vivo. Activation of a specific pool of neurons tends to be trickier than the stimulating all the opsin-expressing cells at the same time, as targeting multiple small areas almost simultaneously or in a short interval without stimulating any other unwanted regions can be quite challenging [72]. Several ways of dealing with this problem have emerged over time either using a scanning or parallel approach [73].

Scanning approach focuses on changing the excitation spot rapidly to stimulate multiple target sites. These transitions are usually achieved by redirecting the light by a certain
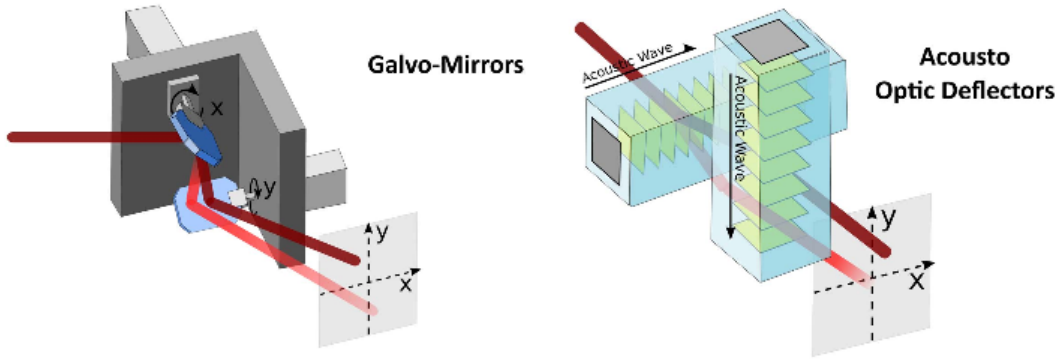
Figure 1.12: Example of scanning approach on multiple target stimulation (taken from Ronzitti et al., 2017 [73]).

angle and scanning over specific trajectories over the sample. A laser is generally used as the light source in this approach, and either acousto-optic deflectors or galvanometer is used to direct the rays to respective stimulation sites [74, 75]. Acousto-optic deflector utilizes acoustic frequency and galvanometer uses mirror controlled by electric current deflect the light beam to the intended target. However, this method has the disadvantage of having a slight time lapse between multiple target sites, which can compromise the temporal resolution. Also, because light passes over other neurons in this approach, an unwanted response may be triggered. Therefore the target sites that should be triggered needs to be within a certain distance, or it may be difficult to achieve a reliable resolution. Therefore this method is more suitable for when the intended targets are closer together and have fewer neurons to stimulate [73, 76].

Parallel approach utilizes patterned light to stimulate multiple sites at once. Example of this approach includes micro-light-emitting diode (micro-LED) array, digital multi-mirror device (DMD), and liquid crystal spatial light modulator (LC-SLM). Micro-LED array turn the corresponding LED on and off to make the pattern, and DMD and LC-SLM each use either mirror or LC to deflect or block the light where it is not needed [77, 78]. This approach has the advantage of having a high spatial resolution with typical DMD having 10^6. The
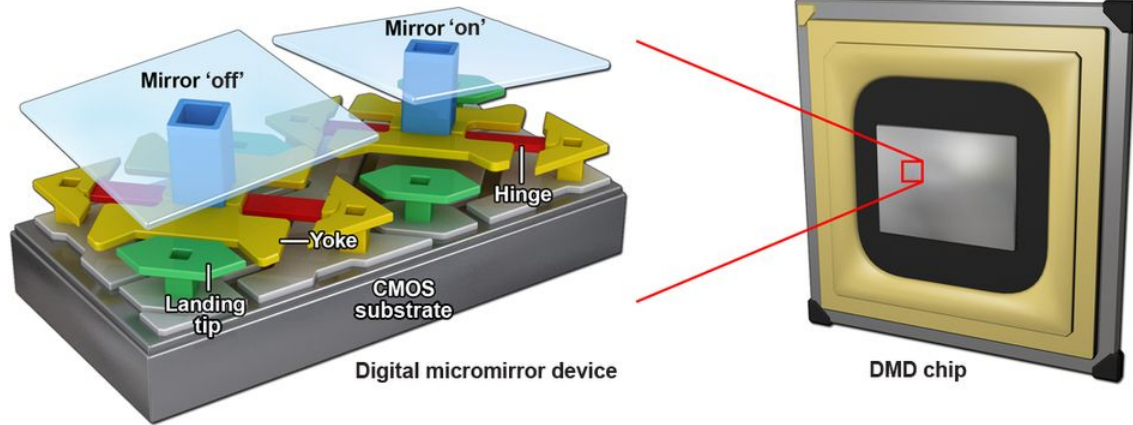
Figure 1.13: Example of digital multimirror device (taken from Allen, 2017 [79]).

temporal resolution that can be achieved using DMD depends on the controller. Currently, DMD with up to 2560x1600 is commercially available which, with the appropriate optical system in place, can achieve a very high spatial resolution. It also utilizes a variety of light source other than laser such as LED which is cheaper as well as more portable. As most of the projectors that have DMD installed has multiple LEDs, a multicolor experiment can be performed relatively easily. [73, 79].

DMD device had been used in multiple optogenetic studies both in vitro and in vivo due to its ability for patterned photostimulation and its high temporal resolution that can reach several kHz [80]. This high spatiotemporal resolution is especially useful when tracking and targeting cells on a live animal such as *Caenorhabditis elegans* [81]. Therefore, the projector that utilizes a DMD device is expected to be able to have higher spatiotemporal resolution compared to other methods mentioned above.

1.5   Research Goals and Approach

To improve upon the current method that uses patch clamp or MEA, we designed a device that incorporates digital light processing (DLP) projector to MEA to combine the

advantages of two different methods; i.e., stimulate and acquire data from multiple neurons at once with high spatiotemporal resolution. To elaborate, compared to the patch clamp that can record from less than 20 neurons at once, MEA provides a better overall picture of the network activity of cultured neurons by recording responses from up to 120 neurons that are located on top of each electrode. Electrical cross-talk that is frequently observed in MEA stimulation is mitigated in this device by utilizing light to stimulate the neurons. DLP projector provides a high temporal resolution of up to 1kHz with a good spatial resolution of around 4μm by 2μm per pixel. Using DLP projector is also advantageous in that it can change the color of the light source quite quickly as it uses a parallel approach for light delivery.

Light from the projector is propagated to the neurons cultured on top of the MEA via simple optics system consisting of two doublet lenses and an objective lens. When the light stimulates the neurons, MEA is able to acquire the electrical response that can be analyzed. As this device is expected to have better spatial resolution when receiving a response from multiple neurons than systems that only use MEA, it is expected to allow closer observation of neural network activity. This increased resolution could lead to a deeper understanding of the influence individual neurons have over the neural circuit and their potential role in the network function.

The objectives of this research effort include the following goals:

1. Deliver the light with high spatial resolution,
2. Synchronize data collection with the light delivery,
3. Collect and process data from the cultured neuron on MEA

The optical system was designed to demagnify the patterned light from the projector.

These patterns are designed beforehand to stimulate each electrode that is on the array both individually and as a combination with other electrodes. The photodiode was placed to act as a trigger for the software with which the data from electrode array is collected and by doing so synchronize the time the light arrives at the target site and allow the time signal appears on the data acquisition software.

Chapter 2

Building and Validation of the Device

2.1 Overview of the General Design

The general design for the device consists mainly of two parts: light delivery and data acquisition. The primary focus was on the light delivery part of the device, as that needs to be in place before any culturing the neuron for the experiment to start.

2.1.1 Optical system

Optical system consists of a DLP projector, two doublet lenses to collimate the light, mirror, and objective lens (For specification of the parts, see Appendix A.1 and A.2). All of these components are aligned on the aluminum rail to allow for customization, and the lens stands are screwed in place using washers that were designed as a cylinder to allow the lenses to turn after it was secured in place. This was an essential feature for the correct alignment of the lenses as the washers that were used before was rectangular, which prevented us from adjusting the lenses to face the light source at a correct angle. The mirror at the edge
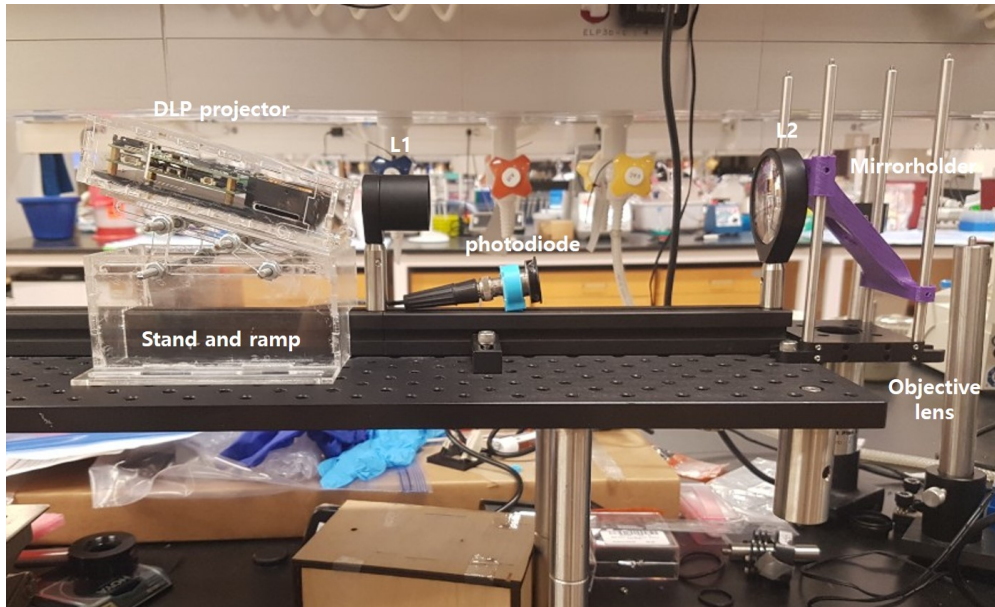
Figure 2.1: Actual setup.
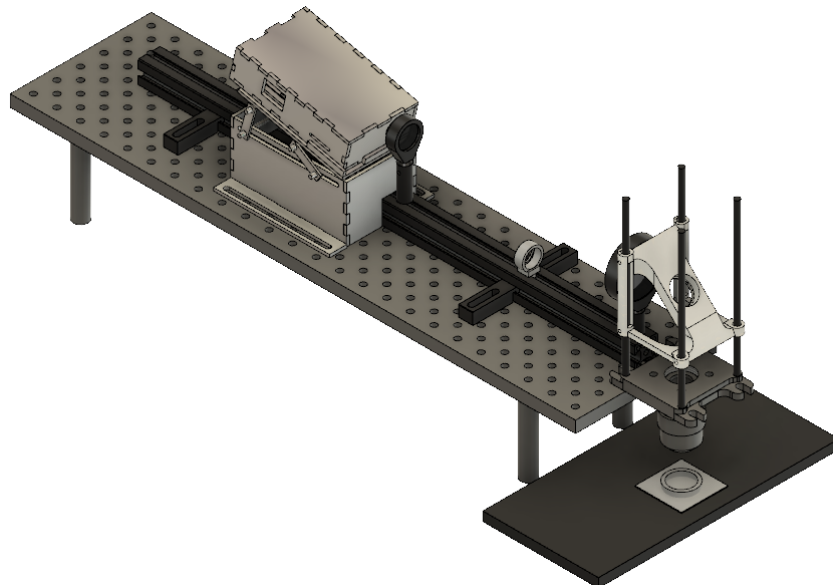
Figure 2.2: Full setup simulated.

directs the light down towards the objective lens, which in turn demagnify the light so that the image is small and intense enough to stimulate neurons individually. To place the optical component correctly, Dr. Gordon Kennedy, who is an optics specialist at Beckman Laser Institute (BLI), provided guidance on the overall structure.

Equipments

1. DLP projector(Texas Instruments (TI). model: DLP LightCrafter Evaluation Module)

2. Ø1" Achromatic Doublet, SM1-Threaded Mount, f = 35mm, ARC: 400-700nm (Thorlabs, model: AC254-035-A-ML)

3. Ø2" Achromatic Doublet, SM2-Threaded Mount, f = 200mm, ARC: 400âĂŞ700nm (Thorlabs, model: AC508-200-A-ML)

4. Achromatic Doublet (f=200.0mm, Ø1", ARC: 400-700nm)

5. Long working distance objective lens(MLWD-5X Long Working Distance Microscope Objective Lens)

6. Mirror (Ø1") Protected Silver Mirror, 0.24" (6.0mm) Thick (Thorlabs, model: PF10-03-P01)

7. Lens Mount with Retaining Ring for Ø1" Optics, 8-32 Tap (Thorlabs, model: LMR1)

8. Lens Mount with Retaining Ring for Ø2" Optics, 8-32 Tap (Thorlabs, model: LMR2)

9. Aluminum Breadboard 8" x 24" x 1/2", 1/4" - 20 Double-Density Taps Threaded Mount, ARC: 400-700(Thorlabs, model: MB824)

10. Vertical Cage System Mounting Plate (Thorlabs, model: CPVM)

11. Cage Assembly Rod, 6" Long, Ø6mm(Thorlabs, model: ER6-P4)

12. 9" and 12" Long Construction Rail(Thorlabs, model: XE25L09, XE25L12)

For the DLP projector, a stand and a ramp were built to have the projector on the specific height and angle. Both of the components were made with laser-cut acrylic. The ramp's angle can be adjusted with the eight bolts that are used to fasten the platform in
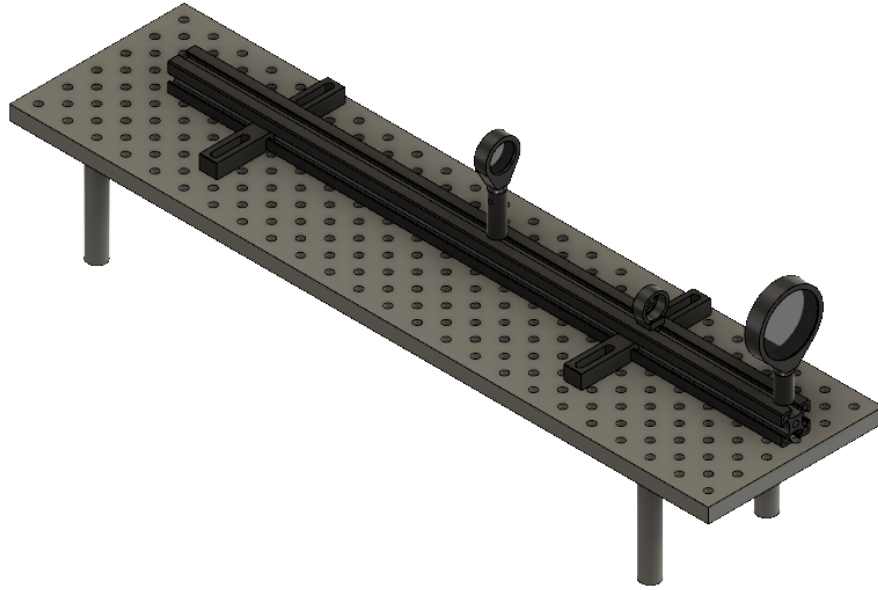
Figure 2.3: Optical components on rail.
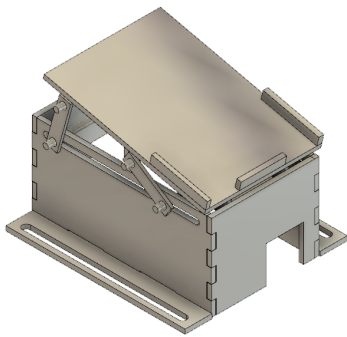
Figure 2.4: DLP projector stand.
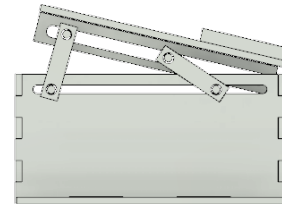
Figure 2.5: Side view of the ramp.
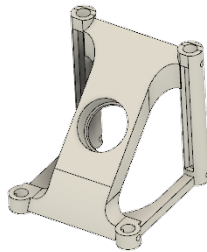
Figure 2.6: Design of mirror holder
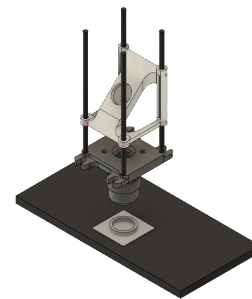
Figure 2.7: Placement of mirror holder in the assembly

place.
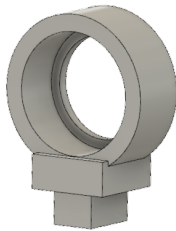
Figure 2.8: Design of photodiode holder.

Figure 2.9: Printed photo diode holder
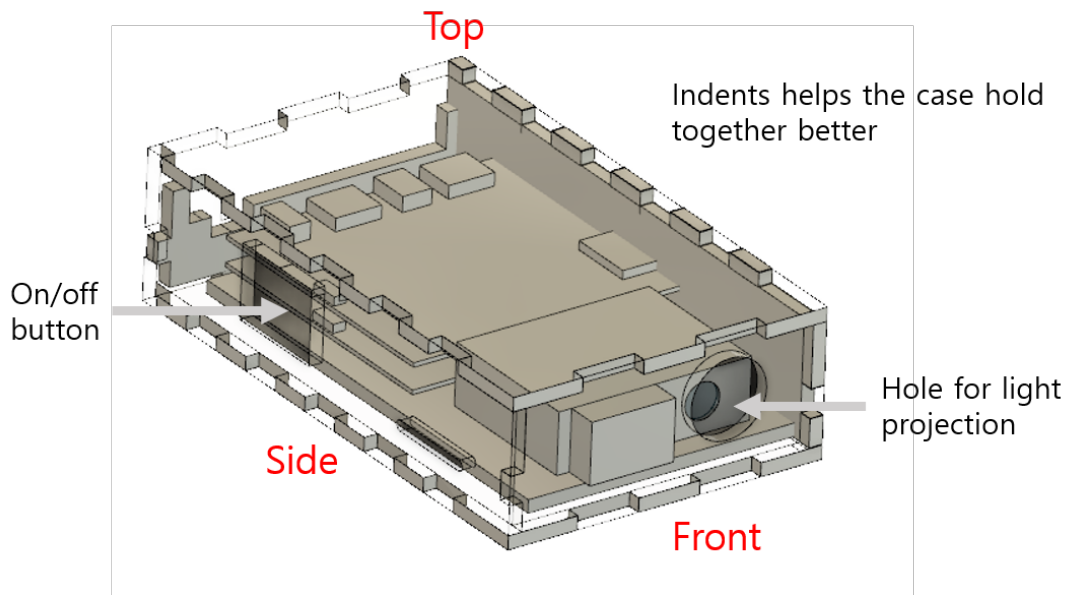
Figure 2.10: Case formation with the DLP projector in place.

To make the adjustment of optics component easier on the rail, round washers were made by laser cutting acrylic sheet with the thickness of around 4mm and was threaded using the threading tool to make it compatible with the screws. Mirror holder and photodiode holder were designed and 3D printed with polylactic acid (Fig. 2.6, 2.8).

2.1.2 Light Pattern Delivery

As the device needs to target the electrode array without requiring a microscope, the default light pattern has 120 rectangles that are associated with each electrode. The

image that is projected with the DLP projector is horizontally elongated as it takes 608 x 684 image to produce an HD image. Therefore, each rectangle that targets an electrode should have approximately 2:1 height to width ratio.

In addition to adjusting the light ray to converge, the demagnification ratio needs to be determined. The size of the rectangles was calculated using the size of an image produced on the target site using a solid pattern that uses all 608 x 684 pixels, which was measured to be about 2.8mm by 5.1mm. From that measurement, pixels that are needed to cover one electrode was determined to be 7 by 4 pixels, which translates to 30 by 30 square microns. Depending on which electrodes are stimulated, the pattern is made using the custom python script.

The frequency at which the light is delivered to stimulate the neurons is controlled by the DLP Lightcrafter graphical user interface (GUI). Multiple bits and multiple color (MBMC) sequence are explicitly used to deliver the light as needed (Appendix B.2). For validation, a sequence provided by the TI which consists of 25 1-bit images with 2225 ms exposure time was used, and the LEDs used for this sequence is red, green, and blue. Red and green LED are only used once each at the beginning, while the rest of the sequence all uses the blue LED.

2.1.3   Data acquisition

As shown in Fig. 2.12, two primary devices for two different functions (light projection and data acquisition) are both connected to the computer but is not physically connected to each other. Also, it is difficult to measure the exact lag between the projector and the computer when the command is given to initiate light pattern sequence. Therefore, it is mandatory to have a way to synchronize the starting point of data acquisition and the starting point for the light sequence. This was achieved by connecting a photodiode to the

27
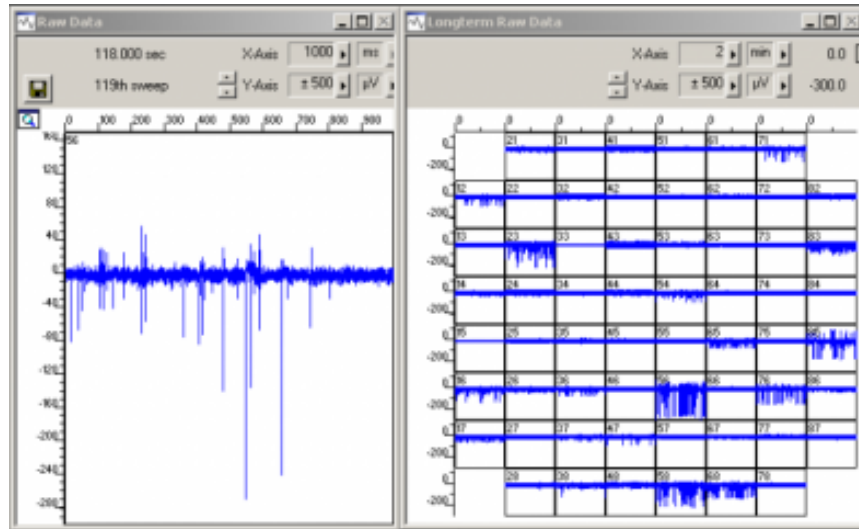
Figure 2.11: Example provided by Multisystem on MC_Rack software use (taken from MC_Rack manual by Multisystem, 2013 [82]).

MEA-2100 system via analog input to record the light intensity as the sequence starts and aligning that data to mark the starting point of the light pattern sequences (see Appendix A.3 for specifications on the device).

After the light stimulates the neurons that are targeted, the electrical response is recorded via the electrode array, which in turn conveys the activity information to the data acquisition device. MEA-2100 has an associated software called MC_Rack (Fig. 2.11) that is provided by MultiSystems which can record the acquired data as analog or digital input and manage properties such as rate of recorded sample per millisecond or threshold for the trigger. The data collected via MC_Rack are pre-processed using MEA tools which converts the data into the format that can be opened on Matlab. The necessary Matlab scripts to analyze the data are also provided by the manufacturer.

Equipments:

1. MEA-2100 systems, including headstage and interface board (MCS-IFB 3.0 Multiboot) (Multichannel systems)

2. 120 electrode array (Multisystems, model: 120MEA200/30iR-Ti-gr)

28
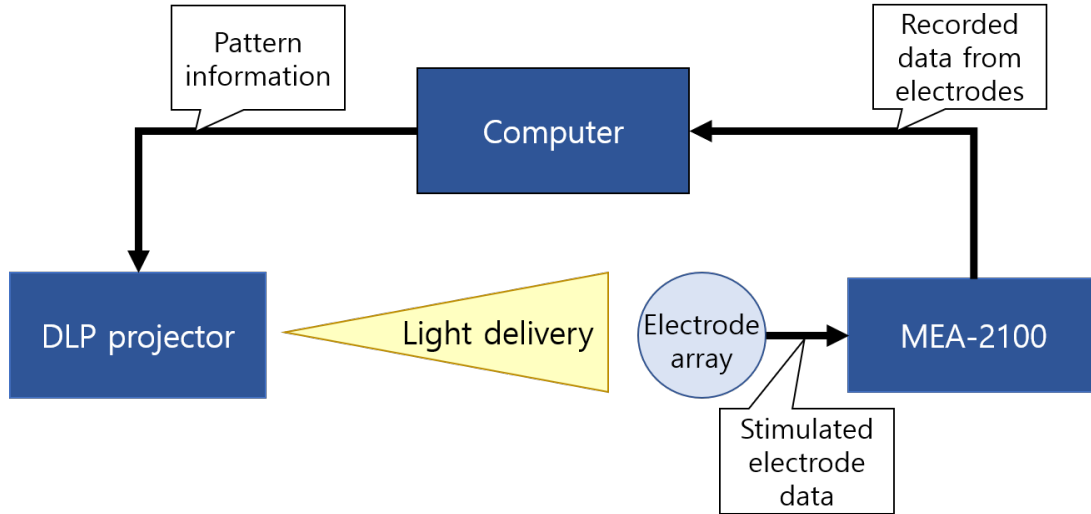
Figure 2.12: Simplified data flow scheme.

3. Silicon photodiode with BNC Connector (Meredith Instruments, model:SD 444-12-12-171)

4. Coaxial Cable, BNC to L00 (Lemo 00 compatible)(BL00-174LN-2)

5. Neutral Density Filter, ND400 49mm (GTX Filters, model: GTX MC-X ND400)

Neural density filter was attached to the photodiode to protect the MEA-2100 system from receiving overly intense light, which may damage the sensitive amplifiers within the device. According to the manufacturer, the ND filter used for this set up reduces light transmission by 1/100. The maximum voltage that the MEA-2100 can manage is 500mV according to the spec sheet. Therefore, the light intensity at solid light and at when 120 electrodes are lit up was measured to make sure that the voltage induced by the light from the photodiode does not exceed that limit.

The sequence begins with a solid pattern of light to initiate a response. This allows us to be able to always get a reliable light intensity for the device to use as a trigger that is used to synchronize the light sequence to the data after recording.
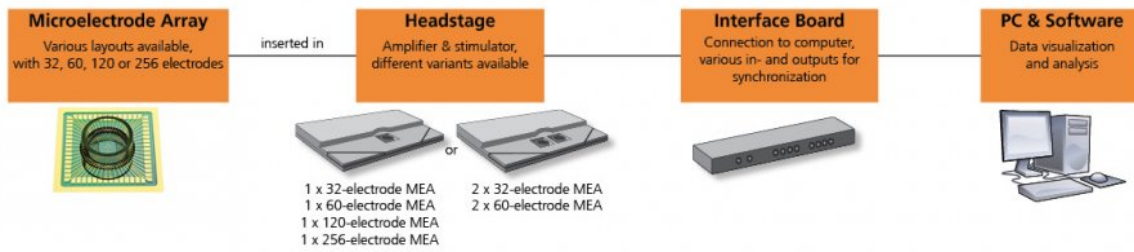
Figure 2.13: MEA-2100 system (taken from multisystems webpage [44]).

2.2 Experimental Procedures

, In order to conduct neural network activity study, genetically modified neurons should be cultured on MEA at least three weeks prior to the day of the experiment. This allows time for the neurons to form a network among themselves and maximize the connection properly. The procedure used for this experiment should follow the previously established method [83]. This culture can be used for up to 3 weeks.

After placing the electrode array on MEA-2100 system, The placement of the electrode array is determined by using a test pattern that targets the four reference electrode that are on the four corners on the array (A1, A12, M1, M12 electrodes marked "ground" on Fig. 2.15).
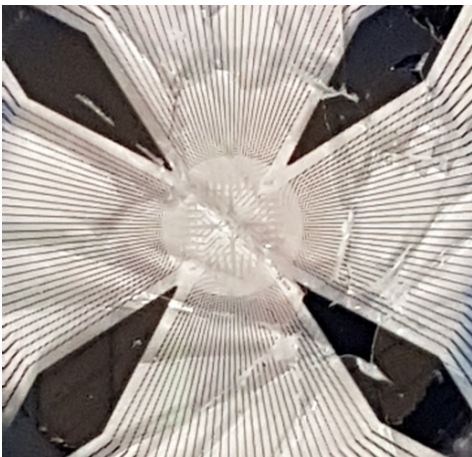
Figure 2.14: Electrode array
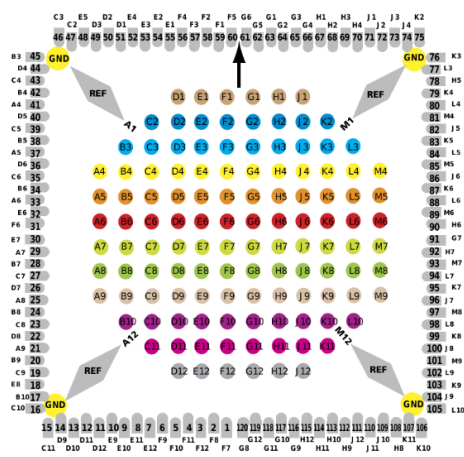
Figure 2.15: Electrode formation.

Light pattern is determined and sent to the DLP projector via computer. All pattern targets one or more electrode locations and stimulates the neurons that are cultured on top of the electrode. Due to the device using a different approach with light instead of an electrical stimulus, parameters for optical stimulation in the cultured neurons need to be optimized. The parameters that need to be determined include light intensity, duration, frequency, and patterns with which to stimulate electrodes. To optimize the intensity of the light, a train of 3 to 5 pulses of light with 5 ms duration are propagated on a single electrode to induce responses as per the previous study utilizing a DLP projector [40]. After the intensity has been determined, the duration should be tested with the same train of 3 to 5 pulses, only this time changing the duration of the pulses. These parameters are then used to determine the frequency. The standard stimulation sequences, such as high-frequency stimulation or theta-burst stimulation sequence, should also be tested as they are often used in other studies that involve stimulating neurons.

After optimizing the parameters, each electrode are stimulated individually, and neural activity from all 120 electrodes are recorded to observe the effect the neuron on that particular electrode has on the culture as a whole. Evoked spikes from the electrodes are recorded and analyzed after the recording. Through the analysis, the electrode that had the most influence over all other electrodes can be determined. For the next step, a combination of two electrodes should be tested for their influence over the culture, and also whether the first electrode that was shown to have invoked the most activity still acts as a significant influence when combined with other electrodes. These experiments continue until the best electrode or electrodes that can activate the network of neurons the most are found. The same experiments should be performed both on wildtype and modified neuron culture to assess the effect of light stimuli on neurons.

Chapter 3

Results

3.1 Final Design

Because the light from DLP projector diverges by default, the optical system first needs to direct the light to collimate. For this purpose, the first lens (L_1) is placed right in front of the DLP projector and the second lens (L_2) at around 23.5cm, i.e., the distance between L_1 and L_2 is the sum of each focal lengths of the two lenses (Fig. 3.2).

After the parallel light hits the mirror, it passes through the objective lens that is placed below. The resulting image is projected 4cm away from the objective lens. Because the light going into the objective lens is parallel, the distance between the L_2 and the mirror does not matter as much as the distance between L_1 and L_2. However, to minimize the size of the device, L_2 is placed near the edge of the breadboard.

DLP projector has an intrinsic 100% offset that makes its image project upwards. This offset serves the purpose of being able to project the entire image from top to bottom while placed on a flat surface. Although a necessary adjustment in terms of a regular
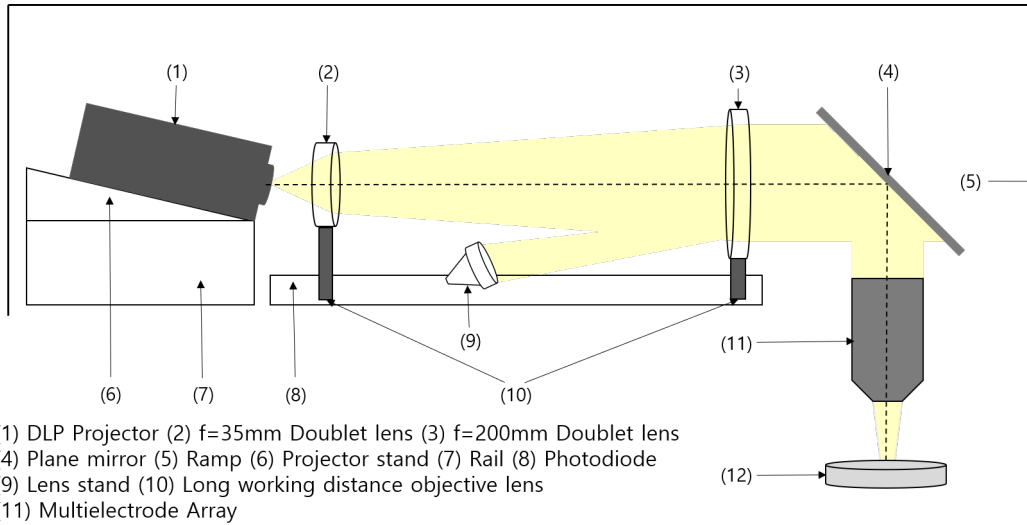
Figure 3.1: Final structure of the device. The light is marked in yellow to show how the it should be directed.

(1) DLP Projector (2) f=35mm Doublet lens (3) f=200mm Doublet lens
(4) Plane mirror (5) Ramp (6) Projector stand (7) Rail (8) Photodiode
(9) Lens stand (10) Long working distance objective lens
(11) Multielectrode Array
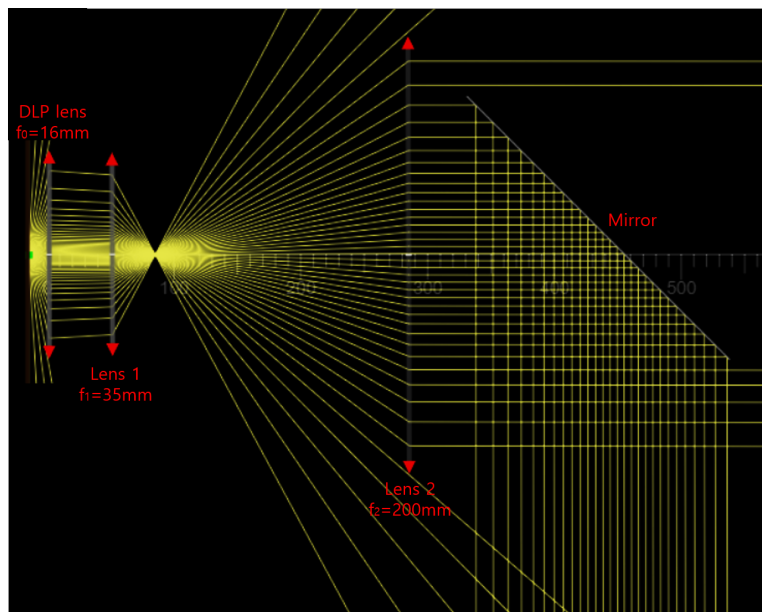
Figure 3.2: Light projection simulated using "Ray Optics Simulation" [84]

projector, this is not useful for the current experiment and should be corrected to minimize the aberration at the target site. This was done by placing the DLP projector at a 13 °angle for the image to enter the L_1 without the offset (Fig. 3.3).

To minimize the effect of ambient light, a large dark box was used to cover the whole optical system to enhance the signal to noise ratio (Fig. 3.1). Not only does this decrease
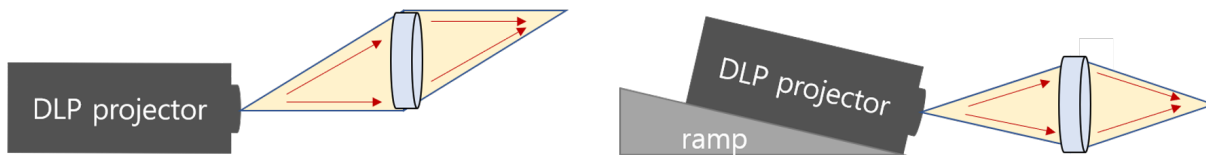
Figure 3.3: Comparing light between when DLP projector is on flat surface or at an angle

the possibility of ambient light corrupting the signal captured by neuron cultured on MEA, but it also enhances the signal to noise ratio for the photodiode. This allows the small amount of light reflected off of L_2 to elicit a response from MEA-2100 effectively without needing another component such as mirror or beamsplitter to direct additional light to the photodiode.

3.2 Light Delivery Validation

The intensity of the light delivered at the target site was measured using a laser power meter (Liconix model 45 PM) in an ambient lit room. Solid light pattern, as well as 120 electrode pattern on Fig. 3.5 was used because that is the maximum amount of light that should be used for the experiment. The result showed 4mW for solid blue light and 0.08mW for 120 electrode pattern. Since light intensity is calculated as power divided by area, the intensity comes out to be 0.4mW/mm^2 when using solid blue light pattern and 0.93mW/mm^2 when using 120 electrodes pattern. Since typical light intensity used for neuron stimulation is 1mW/mm^2, this device is expected to be able to stimulate the neuron using the current set up [85].

According to the DLP Lightcrafter manual, the full-on full-off contrast should be 685:1. However, when the full-off image (i.e., black image) was measured with the power meter, the measurement was 0.015mW, which calculates out to about 266.67:1. This lower contrast ratio probably would have been due to the existence of ambient light in the lab, as

the ambient light was close to 0.013mW.

The wavelength of the three LED light in the DLP projector was measured in the previous study to ensure that the wavelength is within the range that can be used to stimulate the appropriate neuron [86]. To check for the actual wavelength of the LED lights installed in the DLP projector, static solid images of red, green, and blue was projected on an OceanView spectrometer in a dark room. Red LED was measured at 620nm, green at 510nm, and blue at 460nm (Fig. 3.4. Y-axis in the image marks the light intensity as "counts", i.e., how many times voltage was induced by the certain wavelength of light). Although somewhat on the lower side, the wavelengths were still within the range of expectation and was consistent over repetition.

A python code that can create the pattern that is needed for the experiment was written by Christian Park (see Appendix B.1 for the full version of the code). The code takes multiple electrodes (e.g., d3, g2, g4) as arguments and provides a bitmap image with the pattern that light up the position of those electrodes (Fig. 3.7). To check for the intensity and shape of the 120 electrodes image, the pattern was projected (Fig. 3.5) into the CCD camera (Q Imaging Retiga EXi, Cooled Mono 12-bit). 3.0 ND filter was used in the optical path to protect the camera from too much exposure.

3.3   Device Synchronization

The photodiode was placed in the rail to capture the light that is reflected off of L_2 and elicit a response according to the light intensity. Before placing the photodiode and measuring the signal from the MEA-2100 device, it is vital to make sure that the light intensity is not too high that it damages the device, as the device contains highly sensitive amplifiers that can be overloaded if the photodiode generates too much current.
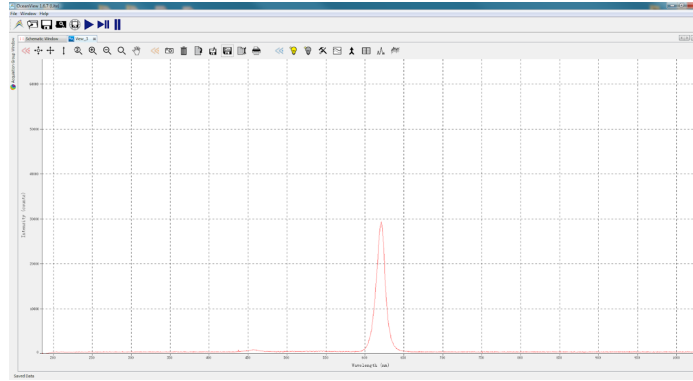
(a) Red LED
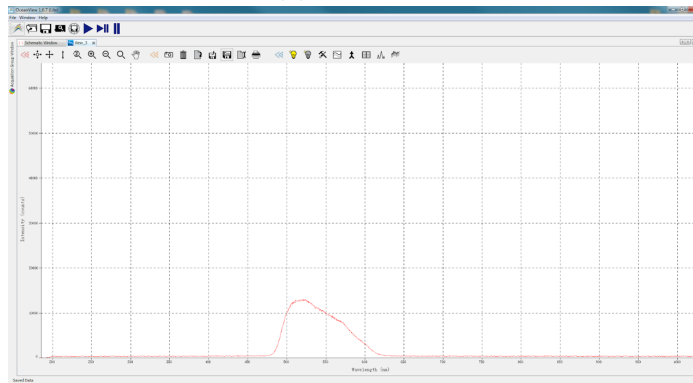
(b) Green LED
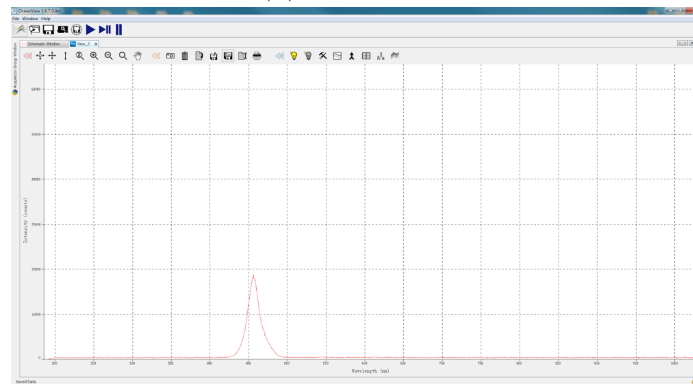
(c) Blue LED

Figure 3.4: Wavelength of three LED in DLP projector.

The photodiode was connected to an oscilloscope to measure the voltage induced by either ambient light, solid blue light, or 120 electrode pattern (Fig. 3.8). The voltage was measured with photodiode placed at the location where MEA should be situated.

According to the spec sheet for MC_Rack, the voltage from the photodiode should be
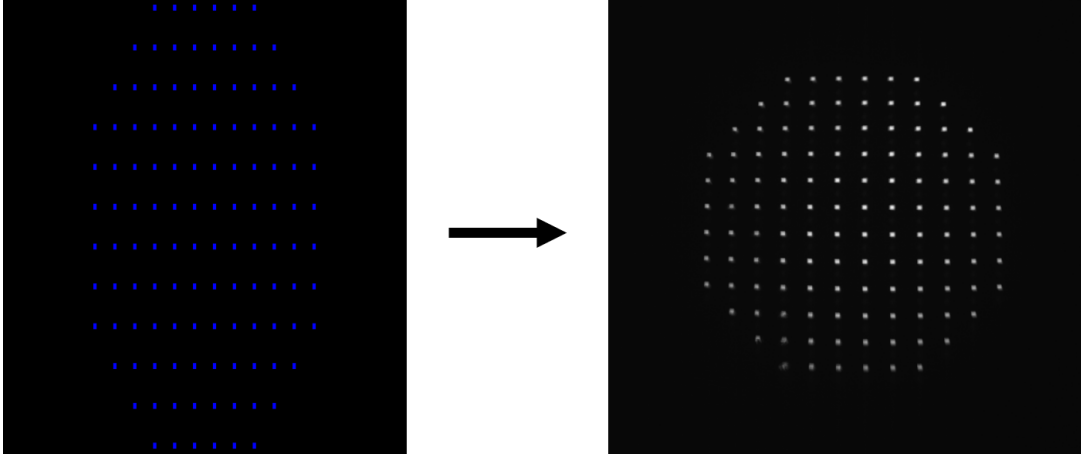
Figure 3.5: Input 120 electrode image and the resulting image
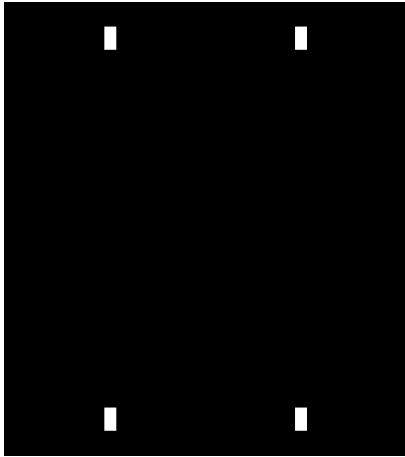
Figure 3.6: Test code for electrode placement.
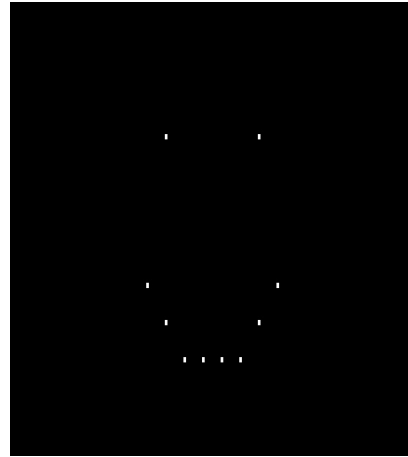
Figure 3.7: Pattern made with the code

lower than ±500 mV. When measured with an oscilloscope, the ambient light was measured to be around -300 mV while the solid blue light and 120 light pattern produced around -420mV and -320mV respectively. As this seems slightly high, the ND filter was included to reduce the light reaching the electrode array. During the measurement, the ND filter was placed right after the L_1 (Fig. 3.1) as the ND filter was quite large could not be placed elsewhere without disrupting the optical system.

After applying ND filter of 2.0 magnitude, the voltage from the photodiode decreased from -410mV to -270mV, which is about 140mV decrease in amplitude. Considering the fact
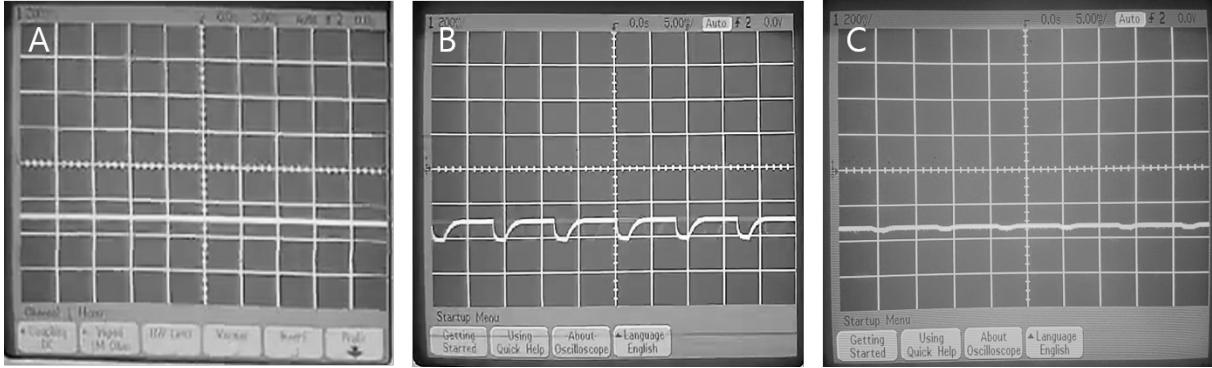
Figure 3.8: Oscilloscope reading of A) ambient light, B) solid blue light, and C) 120 electrode pattern at the MEA location.
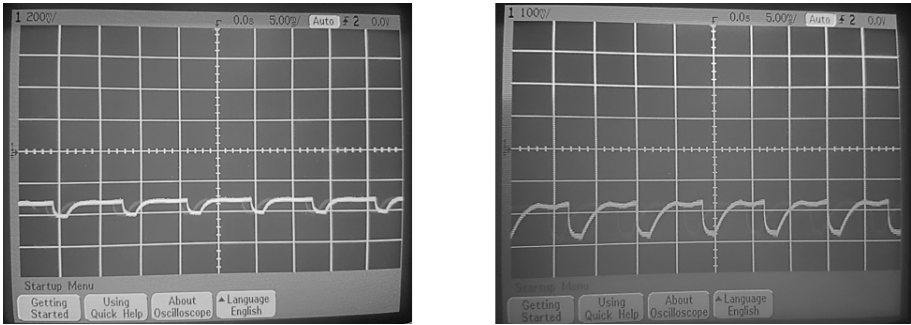
Figure 3.9: Oscilloscope reading of 120 electrode pattern without ND filter (left) and with ND filter (right). As the peaks were getting smaller, the reading on the right uses the 100mV grid as opposed to 200 mV grid on the left.

that the intensity was around -320mV at the target site, the photodiode is expected to generate around -180mV of light in the actual experiment. As that seems low enough not to damage the MEA-2100 device, ND filter was cut to an appropriate size and attached to the front of the photodiode using double-sided tape.

As the solid light pattern is to be used to trigger a response from the photodiode, each LED light on the DLP projector was measured via MEA-2100 to determine which one suit the purpose the best. After observing the intensity of both red and green LED, the red LED was decided. Although red LED showed a weaker signal than the green LED, its wavelength is further away from blue in the light spectrum and is generally less toxic to the cell [87]. Therefore it is expected to provide enough light to elicit a response for the photodiode while having minimal effect on the neurons.
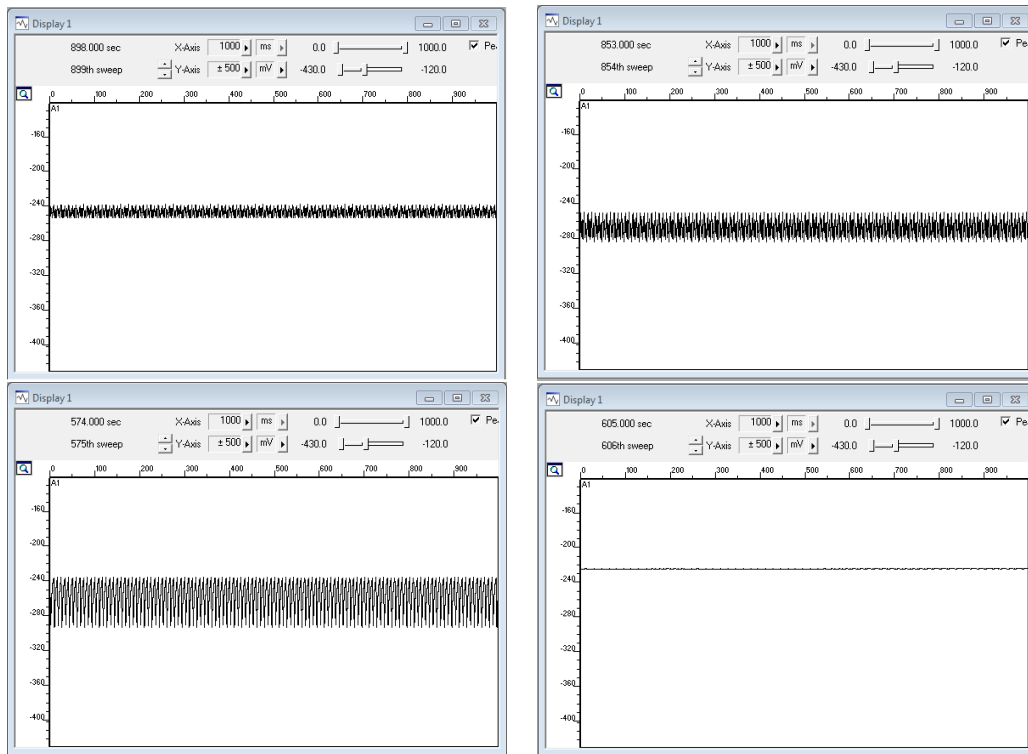
Figure 3.10: Photodiode reading from MC_Rack on red (upper left), green (upper right) blue (lower left) and black (lower right).

After a solid red pattern was assigned on the test sequence, the signal from the
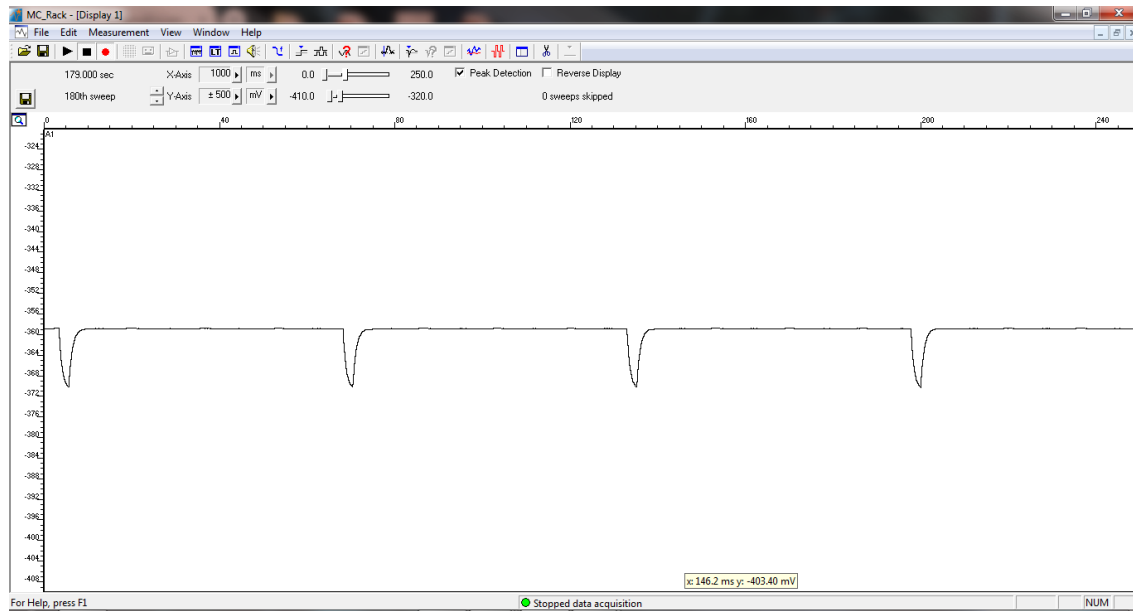
Figure 3.11: Repeating pattern display.

sequence was monitored using long term display. As the pattern repeated itself, the spikes were observed where the red solid pattern came back around (Fig. 3.11). By setting the trigger threshold at somewhere between the lowest point and the middle point of the red pattern intensity, the trigger marker showed up on the long-term display. In the actual experiment setting, the recording includes the reading from the dead time before the trigger as well as all the signal captured after it (Fig. 3.12). The trigger marker is shown on the F6 on when observing long term display on the 120 electrode data (Fig. 2.11).
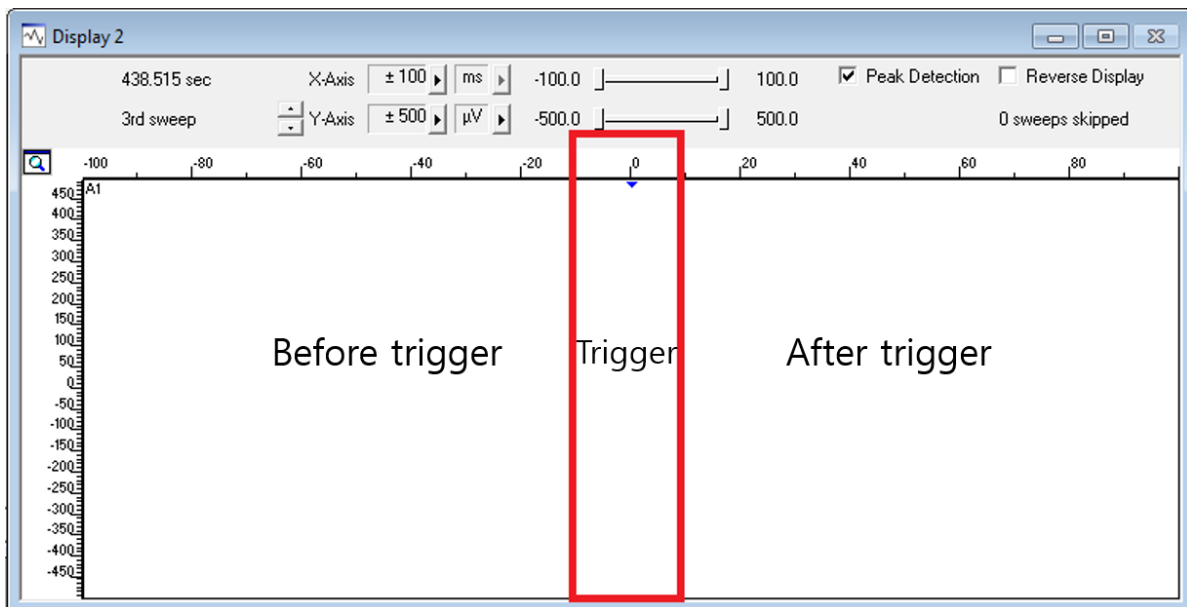
Figure 3.12: Example of trigger marked on to the display.

Chapter 4

Discussion and Future work

4.1 Future experiments to be conducted

Although the contrast ratio of the device when all or no mirror are on was measured, the ratio when only some part of the DMD is activated was not able to be determined by the current power meter. This contrast ratio can be measured by utilizing an appropriate CCD camera to capture and process the image. For this experiment, it is mandatory to calculate the contrast ratio of lit up electrodes and the space between the neighboring electrode to make sure that the light that reaches the interval is not strong enough to induce a response.

It is well known that light, especially blue light, is toxic to the neurons and other cells as it induces cellular damage [88, 89]. Therefore it is important to understand exactly how much light can be applied before the sample is no longer usable and how to minimize that effect so that the sample could be used as long as possible. Some of the strategies of reducing the phototoxicity include increasing the spatial resolution to lower the unnecessary photodamage to the neurons around the actual target and making the exposure time shorter [90]. These factors should be taken into account during the optimization of the parameter

stage of the experiment.

Because the device targets a single layer of neurons, light scattering within the tissue should not be a major concern. If the higher light intensity is required, however, the light scattering that occurs in the optical path could be an issue. There are several ways to mitigate this; change the two doublet lenses that are currently used to collimate the light, alter the position of the projection lens inside the projector itself to prevent light from diverging, or building a new custom projector that utilizes DMD and LED but does not have a projection lens to diverge the light.

Similar to the electric artifact that occurs with an electrode, a light stimulus is known to have its own potential noise that can interfere with the signals. Both photovoltaic and photoelectric effect has been discussed as a possible interfering factor [91, 92]. The LFP recording from silicon-substrate electrodes was found to produce spike-like artifacts that can easily be mistaken for hippocampal oscillation caused by the photovoltaic effect [92]. Similarly, the photoelectric effect was observed in electrophysiological data and corrupted the signal acquired from the electrodes [91]. However, most reports on both effects are from in vivo stimulation, which requires higher intensity and often has the light source placed very close to the sample itself. This can increase the number of photons per second that reaches the electrode, which increases the likelihood of the artifacts. Although the current device has the light source further away than the usual in vivo optogenetic experiment, an experiment with the electrode with and without the neurons needs to be performed in order to determine the best distance for the light source that does not cause too many artifacts but still elicits a response from the appropriate neurons. Other methods of mitigating the issue of optical artifacts include changing the material of the electrodes or the opsin protein to have the neurons react to longer wavelength [91, 92].

4.2 Limitation of current device

One of the advantages of this device is that it can be used without a microscope. However, for this to be viable, the array and the MEA-2100 system must always be at a specific location where the light stimulates the correct electrodes. Therefore, there needs to be a reliable structure that can hold the MEA-2100 system at a specific location.

Although MBMC is optimal for utilizing multiple color LEDs and producing controlled patterns, only 96 patterns can be used at most and therefore is not very suitable when the experiment calls for a longer measurement. For this problem, the HDMI port display mode where DLP projector is connected to the graphic card of a computer to act as an external display could be a potential solution. Because it is utilizing the memory from the computer, it does not have a limit on how many patterns it can hold. Therefore it may be more optimal for an experiment that studies network activity over a more extended period of time.

To understand the communication between the hippocampal subregions, the current method of using a single electrode array may not suffice as it is difficult to pinpoint which neuron came from which part of the hippocampus. Therefore, a multi-compartment should be used on electrode array to culture the neurons from different subregions separately. These kinds of the multi-compartment electrode were used previously by Dr. Brewer et al. in 2013 to study self wiring property of the hippocampal subregion [7] (Fig. 4.1). This implies that the hippocampal subregions, even when cultured separately in vitro, retains its unidirectional connection observed in vivo. Therefore it has the potential to show similar network communication between subregions in vitro that can be analyzed to gain a deeper understanding of its mechanism.
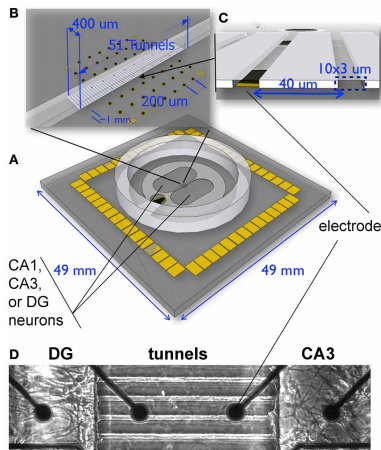
Figure 4.1: Double compartment MEA used for hippocampal subregion network reconstruction in vitro [7]

4.3 Scheme for Animal Testing

The animal study should be conducted in order to test the device in full function. The protocol for the animal experiment was approved in July 2019 by UCI's Institutional Animal Care and Use Committee (see Appendix C.2 for full version of the protocol), and the general procedure is as follows.

For the purpose of the experiment, mice that are already genetically modified to have channelrhodopsin in the hippocampal neuron are used as opposed to using a viral vector to infect the neurons in vitro. This provides a more uniform distribution of modified neuron, which is favorable for the purpose. The strain used for this experiment is Thy1-ChR2-YFP from JAX laboratory. ChR2 was selected as the opsin of choice for this experiment as it is known to be especially effective for inducing an action potential in a neuron, and also because it was used in the previous study by Barral et al. in 2017 [40]. Heterozygous mice are crossed with wildtype mouse to produce pups that are needed for the experiment. The Homozygous mice are discouraged from breeding by the supplier as they may have defects that can negatively affect the breeding.

As the experiment requires only a small number of pups, one or two pair of breeder

mice can be used to obtain the necessary tissue samples. As mice begin to reproduce from around 6-8 weeks of age and are generally used until up to 7-8 months of age, a breeder pair can be expected to produce about four litters until they need to be replaced. As this research requires continued breeding to obtain neural tissue, a pair from the litter should be set aside to let them grow into a new breeder pair if the need arises (Fig. 4.2. All breeder pair should consist of a genetically modified male and a wildtype female, as the pups should be produced in a consistent condition. Also, if the mouse colony needs to become larger in the future, wildtype females are easier to obtain than the modified ones.

The pups should be genotyped as soon as they are born to make sure they have the right genotype before they are sacrificed (see Appendix C.2 for recommended methods). It is vital to get the genotypes as soon as possible because the neurons grow best when the pups are less than five days old [93, 94]. The heterozygous pups should be used as the experimental group, and their wildtype sibling should be used as a control in order to determine the background noise level and calibrate light intensity. Typically one litter consists of 6-10 pups, therefore around 2-5 pups for each genotype are expected to be born. One pup can provide neurons enough to cover around four electrodes as the neurons are expected to be plated with the density of 1000 cells/mm^2. By having mice breed once a month, up to 16-20 cultures per genotype per litter are available. As these pups are very young (P0-P5), putting them on ice for 15 min to induce hypothermia is an acceptable way of euthanasia.

To have a steady number of mice pups without compromising the breeder mice's health, 2 or 3 breeder pairs should be used in turn to obtain the pups. For example, if pair A was bred this month to obtain the pups, pair B should be used next month instead of reusing pair A. This is also beneficial to the current scheme of raising the new breeder pair from the previous litter, as the mother has time to take care of the pups before the pups are weaned at 21 days of age.
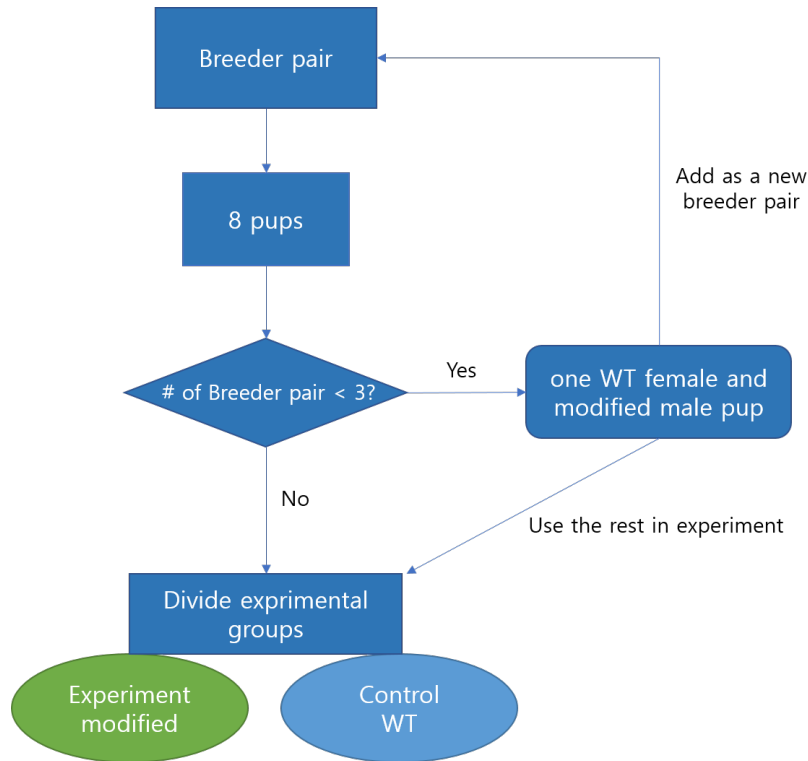
Figure 4.2: Breeding scheme

4.4 Conclusion and future outlook

Brain rarely uses one specific part to perform a complex function; multiple neurons that form neural circuits from different parts of the brain all communicate for an organism to perform a variety of functions. Therefore, it is essential to understand these neural network activities to gain insight into how the brain works as well as how and where it can be damaged.

Through the design and validation of the device, an optical platform was built that uses optogenetics and MEA to achieve high spatiotemporal resolution. The device can target multiple neurons at once without affecting the ones that should not be stimulated by using both optogenetics and MEA. The device is able to capture the network activity of neurons and is expected to provide a way to understand the activity of each neural circuit in hippocampus better.

As this method helps recreate the network activity of neurons in a much more controlled environment and shows a basis of the interaction between a neural network, it can effectively show the fundamental mechanism that makes the hippocampus work. It is especially targeted towards finding the effect each neuron may have over the other neurons to identify the network hierarchy of neural circuit. By incorporating this finding for study on memory formation and neurodegenerative disease, it may be possible to gain new insight on how the disruption of a certain neuron may have a bigger impact on network activity than others and how that can relate to poor memory formation. By establishing the different level of significance over the group of neurons in this device, more studies can be conducted to understand the "leader" of the neural circuit; whether or not they are more susceptible to damage, if the leader was to be damaged which neuron would take its place, and other possible intrinsic characteristics that may differentiate "leader" from "follower" could also be analyzed for comprehending the underlying mechanism of neural circuit.

This device may also be utilized for research associated with drug screening as it strives to replicates the hippocampal neural activity in vitro. In vitro cultures are already being used in fields such as seizure liability testing and, though less common, in memory loss testing [95, 96]. Identifying the leader neuron and observing the effect a particular chemical has on them can be beneficial to finding an effective drug for memory associated disease.

Bibliography

[1] Danielle S Bassett and Olaf Sporns. Network neuroscience. *Nature Neuroscience*, 20:353, feb 2017.

[2] K M Mccullough, F G Morrison, and K J Ressler. Neurobiology of Learning and Memory Bridging the Gap : Towards a cell-type specific understanding of neural circuits underlying fear behaviors. *Neurobiology of Learning and Memory*, 135:27–39, 2016.

[3] Jacob G Bernstein and Edward S Boyden. Optogenetic tools for analyzing the neural circuits of behavior. *Trends in Cognitive Sciences*, 15(12):592–600, 2011.

[4] Stanley Heinze. Neural circuits underlying complex brain function across animals - from conserved core concepts to specializations defining a species' identity - braininbrain - erc. *Impact*, 2018(8):46–48, 2018.

[5] Sarah J. Cohen and Robert W. Stackman Jr. Assessing rodent hippocampal involvement in the novel object recognition task. a review. *Behavioural Brain Research*, 285:105 – 117, 2015. SI: Object Recognition Memory in Rats and Mice.

[6] Daniela J Palombo, Agnes Bacopulos, Robert S C Amaral, Rosanna K Olsen, Rebecca M Todd, Adam K Anderson, and Brian Levine. Episodic autobiographical memory is associated with variation in the size of hippocampal subregions. *Hippocampus*, 28(2):69–75, 2017.

[7] Gregory J Brewer, Michael D Boehler, Stathis Leondopulos, Liangbin Pan, Sankaraleengam Alagapan, Thomas B DeMarse, and Bruce C Wheeler. Toward a self-wired active reconstruction of the hippocampal trisynaptic loop: DG-CA3. *Frontiers in neural circuits*, 7:165, oct 2013.

[8] Danny Eytan and Shimon Marom. Dynamics and effective topology underlying synchronization in networks of cortical neurons. *Journal of Neuroscience*, 26(33):8465–8476, 2006.

[9] U.S. Census Bureau. 2010 Census Summary File âĂŤ Technical Documentation/prepared by the U.S. Census Bureau. 4(September), 2012.

[10] Liesi E. Hebert, Jennifer Weuve, Paul A. Scherr, and Denis A. Evans. Alzheimer disease in the united states (2010–2050) estimated using the 2010 census. *Neurology*, 80(19):1778–1783, 2013.

[11] T S Dharmarajan and Srinivas G Gunturu. Alzheimer's disease: a healthcare burden of epidemic proportion. *American health & drug benefits*, 2(1):39–47, jan 2009.

[12] Jeffrey Cummings, Garam Lee, Aaron Ritter, and Kate Zhong. Alzheimer's disease drug development pipeline: 2018. *Alzheimer's & Dementia: Translational Research & Clinical Interventions*, 4:195–214, jan 2018.

[13] Stephen R Robinson, Holly M Brothers, and Maya L Gosztyla. Consequences of redefining Alzheimer's disease in terms of amyloid burden without regard to cognitive decline. *Neural regeneration research*, 13(12):2098–2099, dec 2018.

[14] Rebekah M Ahmed, Emma M Devenney, Muireann Irish, Arne Ittner, Sharon Naismith, Lars M Ittner, Jonathan D Rohrer, Glenda M Halliday, Andrew Eisen, John R Hodges, and Matthew C Kiernan. Neuronal network disintegration : common pathways linking neurodegenerative diseases. *Journal of Neurology, Neurosurgery & Psychiatry*, 87(11):1234–1241, 2016.

[15] Francesca Mangialasche, Alina Solomon, Bengt Winblad, Patrizia Mecocci, and Miia Kivipelto. Alzheimer's disease: clinical trials and drug development. *The Lancet Neurology*, 9(7):702 – 716, 2010.

[16] Jaume Folch, Dmitry Petrov, Miren Ettcheto, Sonia Abad, Elena Sánchez-lópez, M Luisa García, Jordi Olloquequi, Carlos Beas-zarate, Carme Auladell, and Antoni Camins. Current Research Therapeutic Strategies for Alzheimer ' s Disease Treatment. *Neural Plasticity*, 2016:15, 2015.

[17] Charles A. J. Romanowski and Iain D. Wilkinson. Atrophy: When too much atrophy is too little brain. *Neuroradiology*, 53(1):133, Aug 2011.

[18] Cornelis Blauwendraat, Sara Bandrés-ciga, and Andrew B Singleton. Pathology and hippocampal atrophy in Alzheimer ' s disease. *The Lancet Neurology*, 16(11):862–864, 2017.

[19] Xiaoying Tang, Dominic Holland, Anders M. Dale, Laurent Younes, Michael I. Miller, and for the Alzheimer's Disease Neuroimaging Initiative. The diffeomorphometry of regional shape change rates and its relevance to cognitive deterioration in mild cognitive impairment and alzheimer's disease. *Human Brain Mapping*, 36(6):2093–2117, 2015.

[20] Liana G Apostolova, Amity E Green, Sona Babakchanian, Kristy S Hwang, Yi-Yu Chou, Arthur W Toga, and Paul M Thompson. Hippocampal atrophy and ventricular enlargement in normal aging, mild cognitive impairment (MCI), and Alzheimer Disease. *Alzheimer disease and associated disorders*, 26(1):17–27, 2012.

[21] Michael V. Accardi, Michael K. Pugsley, Roy Forster, Eric Troncy, Hai Huang, and Simon Authier. The emerging role of in vitro electrophysiological methods in CNS safety pharmacology. *Journal of Pharmacological and Toxicological Methods*, 81:47–59, 2016.

[22] Antãşnio J. Bastos-Leite, Wiesje M. van der Flier, Elisabeth C.W. van Straaten, Salka S. Staekenborg, Philip Scheltens, and Frederik Barkhof. The contribution of medial temporal lobe atrophy and vascular pathology to cognitive impairment in vascular dementia. *Stroke*, 38(12):3182–3185, 2007.

[23] Y A L Pijnenburg, F Barkhof, H Josef Gertz, and P Scheltens. Hippocampal atrophy on MRI in frontotemporal lobar degeneration and Alzheimer ' s disease. *Journal of Neurology, Neurosurgery & Psychiatry*, 77(4):439–442, 2006.

[24] Moretti D.V., Pievani M., Geroldi C., Binetti G., Zanetti O., Cotelli M., and Rossini P.M. Increasing hippocampal atrophy and cerebrovascular damage is differently associated with functional cortical coupling in MCI patients. *Alzheimer Disease and Associated Disorders*, 23(4):323–332, 2009.

[25] Usman A Khan, Li Liu, Frank A Provenzano, Diego E Berman, Caterina P Profaci, Richard Sloan, Richard Mayeux, Karen E Duff, and Scott A Small. Molecular drivers and cortical spread of lateral entorhinal cortex dysfunction in preclinical Alzheimer's disease. *Nature Neuroscience*, 17:304, dec 2013.

[26] Alison Goate, D Ph, Nick C Fox, Daniel S Marcus, D Ph, Nigel J Cairns, D Ph, Xianyun Xie, Tyler M Blazey, David M Holtzman, Anna Santacruz, Virginia Buckles, D Ph, Angela Oliver, Krista Moulder, D Ph, Paul S Aisen, Bernardino Ghetti, William E Klunk, Eric Mcdade, Ralph N Martins, D Ph, Colin L Masters, Richard Mayeux, John M Ringman, Martin N Rossor, Peter R Schofield, D Ph, D Sc, Reisa A Sperling, Stephen Salloway, John C Morris, Dominantly Inherited, and Alzheimer Network. Clinical and Biomarker Changes in Dominantly Inherited Alzheimer's Dise. *The New England Journal of Medicine*, 367(9):795–804, 2012.

[27] Latha Velayudhan, Petroula Proitsi, Eric Westman, J-sebastian Muehlboeck, and Patrizia Mecocci. Entorhinal Cortex Thickness Predicts Cognitive Decline in Alzheimer ' s Disease. *Journal of Alzheimer's Disease*, 33:755–766, 2013.

[28] Sarah B. Martin, Charles D. Smith, Heather R. Collins, Fred A. Schmitt, and Brian T. Gold. Evidence that volume of anterior medial temporal lobe is reduced in seniors destined for mild cognitive impairment. *Neurobiology of Aging*, 31(7):1099 – 1106, 2010.

[29] B.C. Dickerson, I. Goncharova, M.P. Sullivan, C. Forchetti, R.S. Wilson, D.A. Bennett, L.A. Beckett, and L. deToledo Morrell. Mri-derived entorhinal and hippocampal atrophy in incipient and very mild alzheimerâĂŹs diseaseâŸĘâŸĘthis research was supported by grants p01 ag09466 and p30 ag10161 from the national institute on aging, national institutes of health. *Neurobiology of Aging*, 22(5):747 – 754, 2001.

[30] Y. Xu, C.R. Jack, P.C. O'Brien, E. Kokmen, G.E. Smith, R.J. Ivnik, B.F. Boeve, R.G. Tangalos, and R.C. Petersen. Usefulness of mri measures of entorhinal cortex versus hippocampus in ad. *Neurology*, 54(9):1760–1767, 2000.

[31] Feng Zhang, Viviana Gradinaru, Antoine R Adamantidis, Remy Durand, Raag D Airan, Luis de Lecea, and Karl Deisseroth. Optogenetic interrogation of neural circuits: technology for probing mammalian brain structures. *Nature Protocols*, 5:439, feb 2010.

[32] Sebastián A. Romano, Verónica Pérez-Schuster, Adrien Jouary, Jonathan Boulanger-Weill, Alessia Candeo, Thomas Pietri, and Germán Sumbre. An integrated calcium imaging processing toolbox for the analysis of neuronal population dynamics. *PLOS Computational Biology*, 13(6):e1005526, jun 2017.

[33] Scott L. Hooper and Joachim Schmidt. *Electrophysiological Recording Techniques*, chapter 2, pages 7–53. John Wiley & Sons, Ltd, 2017.

[34] Vincent G Kokich. In-vitro vs in-vivo materials research. *American Journal of Orthodontics and Dentofacial Orthopedics*, 143(4):S11, apr 2013.

[35] Ratner MH. The Future Role of In vivo Electrophysiology in Preclinical Drug Discovery. *EC Pharmacology and Toxicology*, 2(2):108–109, 2016.

[36] Daniel Keller, Csaba Erö, and Henry Markram. Cell Densities in the Mouse Brain: A Systematic Review. *Frontiers in neuroanatomy*, 12:83, oct 2018.

[37] Chao-Yin Chen. *Patch Clamp Technique and Applications*, pages 49–64. Springer New York, New York, NY, 2017.

[38] Nikolaus J. Sucher, David L. Deitcher, Deborah J. Baro, Ronald M. Harris Warrick, and Elke Guenther. Genes and channels: patch/voltage-clamp analysis and single-cell rt-pcr. *Cell and Tissue Research*, 302(3):295–307, Dec 2000.

[39] Carl C H Petersen. Whole-Cell Recording of Neuronal Membrane Potential during Behavior. *Neuron*, 95(6):1266–1281, sep 2017.

[40] Jérémie Barral and Alex Reyes. Optogenetic Stimulation and Recording of Primary Cultured Neurons with Spatiotemporal Control. *BIO-PROTOCOL*, 7(12), 2017.

[41] Niels Fertig, Robert H. Blick, and Jan C. Behrends. Whole cell patch clamp recording performed on a planar glass chip. *Biophysical Journal*, 82(6):3056 – 3062, 2002.

[42] Guangfu Wang, Daniel R Wyskiel, Weiguo Yang, Yiqing Wang, Lana C Milbern, Txomin Lalanne, Xiaolong Jiang, Ying Shen, Qian-Quan Sun, and J Julius Zhu. An optogenetics- and imaging-assisted simultaneous multiple patch-clamp recording system for decoding complex neural circuits. *Nature Protocols*, 10:397, feb 2015.

[43] Seung-Jae Kim, Sandeep C Manyam, David J Warren, and Richard A Normann. Electrophysiological mapping of cat primary auditory cortex with multielectrode arrays. *Annals of biomedical engineering*, 34:300–9, 03 2006.

[44] Multi Channel Systems. Mea2100-systems.

[45] Ming-Gang Liu, Xue-Feng Chen, Ting He, Zhen Li, and Jun Chen. Use of multi-electrode array recordings in studies of network synaptic plasticity in both time and space. *Neuroscience bulletin*, 28:409–22, 08 2012.

[46] Jacob T Robinson, Marsela Jorgolli, Alex K Shalek, Myung-Han Yoon, Rona S Gertner, and Hongkun Park. Vertical nanowire electrode arrays as a scalable platform for intracellular interfacing to neuronal circuits. *Nature nanotechnology*, 7(3):180–184, jan 2012.

[47] Matthew J. Nelson, Silvana Valtcheva, and Laurent Venance. Magnitude and behavior of cross-talk effects in multichannel electrophysiology experiments. *Journal of Neurophysiology*, 118(1):574–594, 2017.

[48] Wonryung Lee, Dongmin Kim, Naoji Matsuhisa, Masae Nagase, Masaki Sekino, George G. Malliaras, Tomoyuki Yokota, and Takao Someya. Transparent, conformable, active multielectrode array using organic electrochemical transistors. *Proceedings of the National Academy of Sciences*, 114(40):10554–10559, 2017.

[49] J M Kilner, S N Baker, and R N Lemon. A novel algorithm to remove electrical cross-talk between surface EMG recordings and its application to the measurement of short-term synchronisation in humans. *The Journal of physiology*, 538(Pt 3):919–930, feb 2002.

[50] Kutluay Uluç, Gregory C. Kujoth, and Mustafa K. BaÅ§kaya. Operating microscopes: Past, present, and future. *Neurosurgical Focus*, 27(3), 2009.

[51] R Splinter and BA Hooper. *An Introduction to Biomedical Optics*. 2007.

[52] Michael A. Thompson, Julie S. Biteen, Samuel J. Lord, Nicholas R. Conley, and W.E. Moerner. Chapter two - molecules and methods for super-resolution imaging. In Nils G. Walter, editor, *Single Molecule Tools, Part B:Super-Resolution, Particle Tracking, Multiparameter, and Force Based Methods*, volume 475 of *Methods in Enzymology*, pages 27 – 59. Academic Press, 2010.

[53] Osamu Shimomura, Frank H. Johnson, and Yo Saiga. Extraction, purification and properties of aequorin, a bioluminescent protein from the luminous hydromedusan, aequorea. *Journal of Cellular and Comparative Physiology*, 59(3):223–239, 1962.

[54] M Chalfie, Y Tu, G Euskirchen, WW Ward, and DC Prasher. Green fluorescent protein as a marker for gene expression. *Science*, 263(5148):802–805, 1994.

[55] Roger Y. Tsien. The green fluorescent protein. *Annual Review of Biochemistry*, 67(1):509–544, 1998. PMID: 9759496.

[56] Leonhard MÃűckl, Don C. Lamb, and Christoph BrÃďuchle. Super-resolved fluorescence microscopy: Nobel prize in chemistry 2014 for eric betzig, stefan hell, and williamâĂĚe. moerner. *Angewandte Chemie International Edition*, 53(51):13972–13977, 2014.

[57] Michael A. Thompson, Matthew D. Lew, and W.E. Moerner. Extending microscopic resolution with single-molecule imaging and active control. *Annual Review of Biophysics*, 41(1):321–342, 2012. PMID: 22577822.

[58] Myron S. Ignatius and David M. Langenau. Chapter 19 - fluorescent imaging of cancer in zebrafish. In H. William Detrich, Monte Westerfield, and Leonard I. Zon, editors, *The Zebrafish: Disease Models and Chemical Screens*, volume 105 of *Methods in Cell Biology*, pages 437 – 459. Academic Press, 2011.

[59] Ankur Baliyan, Hideto Imai, and Vinit Kumar. Chapter 7 - microscopy. In Gauri Misra, editor, *Data Processing Handbook for Complex Biological Data Sources*, pages 97 – 117. Academic Press, 2019.

[60] Peter T. C. So, Chen Y. Dong, Barry R. Masters, and Keith M. Berland. Two-photon excitation fluorescence microscopy. *Annual Review of Biomedical Engineering*, 2(1):399–429, 2000. PMID: 11701518.

[61] Volodymyr Nikolenko, Kira E Poskanzer, and Rafael Yuste. Two-photon photostimulation and imaging of neural circuits. *Nature Methods*, 4:943, oct 2007.

[62] Xue Han, Xiaofeng Qian, Jacob G Bernstein, Hui-Hui Zhou, Giovanni Talei Franzesi, Patrick Stern, Roderick T Bronson, Ann M Graybiel, Robert Desimone, and Edward S Boyden. Millisecond-timescale optical control of neural dynamics in the nonhuman primate brain. *Neuron*, 62(2):191–198, apr 2009.

[63] Edward S Boyden, Feng Zhang, Ernst Bamberg, Georg Nagel, and Karl Deisseroth. Millisecond-timescale, genetically targeted optical control of neural activity. *Nature Neuroscience*, 8(9):1263–1268, 2005.

[64] Jacob G. Bernstein and Edward S. Boyden. Optogenetic tools for analyzing the neural circuits of behavior. *Trends in Cognitive Sciences*, 15(12):592 – 600, 2011.

[65] E.A. Claudia Pama, Lorenza Colzato, and Bernhard Hommel. Optogenetics as a neuromodulation tool in cognitive neuroscience. *Frontiers in Psychology*, 4:610, 2013.

[66] Kay M Tye and Karl Deisseroth. Optogenetic investigation of neural circuits underlying brain disease in animal models. *Nature Reviews Neuroscience*, 13:251, mar 2012.

[67] Jessica A Cardin, Marie Carlén, Konstantinos Meletis, Ulf Knoblich, Feng Zhang, Karl Deisseroth, Li-Huei Tsai, and Christopher I Moore. Targeted optogenetic stimulation and recording of neurons in vivo using cell-type-specific expression of Channelrhodopsin-2. *Nature Protocols*, 5:247, jan 2010.

[68] Linda Madisen, Aleena R. Garner, Daisuke Shimaoka, Amy S. Chuong, Nathan C. Klapoetke, Lu Li, Alexander van der Bourg, Yusuke Niino, Ladan Egolf, Claudio Monetti, Hong Gu, Maya Mills, Adrian Cheng, Bosiljka Tasic, Thuc Nghi Nguyen, Susan M. Sunkin, Andrea Benucci, Andras Nagy, Atsushi Miyawaki, Fritjof Helmchen, Ruth M. Empson, Thomas KnÃűpfel, Edward S. Boyden, R. Clay Reid, Matteo Carandini, and

Hongkui Zeng. Transgenic mice for intersectional targeting of neural sensors and effectors with high specificity and performance. *Neuron*, 85(5):942 – 958, 2015.

[69] Karl Deisseroth. Optogenetics. *Nature Methods*, 8:26 EP –, Dec 2010.

[70] Bruno Camporeze, Bruno Alcântara Manica, Gabriel Alves Bonafé, Jivago Jordão Camargos Ferreira, Aurélio Lourenço Diniz, Carlos Tadeu Parisi de Oliveira, Luis Roberto Mathias Junior, Paulo Henrique Pires de Aguiar, and Manoela Marques Ortega. Optogenetics: the new molecular approach to control functions of neural cells in epilepsy, depression and tumors of the central nervous system. *American journal of cancer research*, 8(10):1900–1918, 2018.

[71] S B Goncalves, J F Ribeiro, A F Silva, R M Costa, and J H Correia. Design and manufacturing challenges of optogenetic neural interfaces: a review. *Journal of Neural Engineering*, 14(4):041001, may 2017.

[72] Samarendra K. Mohanty and Vasudevan Lakshminarayananan. Optical techniques in optogenetics. *Journal of Modern Optics*, 62(12):949–970, 2015.

[73] Emiliano Ronzitti, Cathie Ventalon, Marco Canepari, Benoît C Forget, Eirini Papagiakoumou, and Valentina Emiliani. Recent advances in patterned photostimulation for optogenetics. *Journal of Optics*, 19(11):113001, oct 2017.

[74] Kaiyu Wang, Yafeng Liu, Yiding Li, Yanmeng Guo, Peipei Song, Xiaohui Zhang, Shaoqun Zeng, and Zuoren Wang. Precise spatiotemporal control of optogenetic activation using an acousto-optic device. *PLOS ONE*, 6(12):1–11, 12 2011.

[75] Michael Kyweriga and Majid H. Mohajerani. *Optogenetic Approaches for Mesoscopic Brain Mapping*, pages 251–265. Springer New York, New York, NY, 2016.

[76] Francesca Anselmi, Arkarup Banerjee, and Dinu F. Albeanu. *Patterned Photostimulation in the Brain*, pages 235–270. Springer International Publishing, Cham, 2015.

[77] Jason Jerome, Robert Foehring, William Armstrong, William J Spain, and Detlef Heck. Parallel optical control of spatiotemporal neuronal spike activity using high-speed digital light processing. *Frontiers in systems neuroscience*, 5:70, 08 2011.

[78] Adam M Packer, Botond Roska, and Michael Häusser. Targeting neurons and photons for optogenetics. *Nature neuroscience*, 16(7):805–815, jul 2013.

[79] John Allen. Application of patterned illumination using a DMD for optogenetic control of signaling. *Nature Methods*, 14:1114, oct 2017.

[80] Seiichiro Sakai, Kenichi Ueno, Toru Ishizuka, and Hiromu Yawo. Parallel and patterned optogenetic manipulation of neurons in the brain slice using a dmd-based projector. *Neuroscience Research*, 75(1):59 – 64, 2013. Photo-transduction proteins and their optogenetic applications in neuroscience.

[81] Andrew M Leifer, Christopher Fang-Yen, Marc Gershow, Mark J Alkema, and Aravinthan D T Samuel. Optogenetic manipulation of neural activity in freely moving Caenorhabditis elegans. *Nature Methods*, 8:147, jan 2011.

[82] Multisystems. *MC_Rack Manual*. Multisystems.

[83] Stefanie Kaech and Gary Banker. Culturing hippocampal neurons. *Nature Protocols*, 1(5):2406–2415, 2006.

[84] Rick Tu Johnson. Ray optics simulation, 2016.

[85] Jonathan Britt, Ross McDevitt, and Antonello Bonci. Use of channelrhodopsin for activation of CNS neurons. *Current protocols in neuroscience*, Chapter2(Unit 2.16), 2012.

[86] Lew Sarah, Huynh Kenny, Chino Iridian, Lopez Alejandra, and Loren Mathew. In Vitro Electrophysiology Platform Using Optogenetic Stimulation. 2018.

[87] Sina Wäldchen, Julian Lehmann, Teresa Klein, Sebastian van de Linde, and Markus Sauer. Light-induced cell damage in live-cell super-resolution microscopy. *Scientific Reports*, 5:15348, oct 2015.

[88] V. Marek, A. Potey, A. RÃľaux-Le-Goazigo, E. Reboussin, A. Charbonnier, T. Villette, C. Baudouin, W. RostÃĺne, A. Denoyer, and S. MÃľlik Parsadaniantz. Blue light exposure in vitro causes toxicity to trigeminal neurons and glia through increased superoxide and hydrogen peroxide generation. *Free Radical Biology and Medicine*, 131:27 – 39, 2019.

[89] John H Stockley, Kimberley Evans, Moritz Matthey, Katrin Volbracht, Sylvia Agathou, Jana Mukanowa, Juan Burrone, and Ragnhildur T Káradóttir. Surpassing light-induced cell damage in vitro with novel cell culture media. *Scientific Reports*, 7(1):849, 2017.

[90] Jaroslav Icha, Michael Weber, Jennifer C. Waters, and Caren Norden. Phototoxicity in live fluorescence microscopy, and how to avoid it. *BioEssays*, 39(8):1–15, 2017.

[91] Takashi D Y Kozai and Alberto L Vazquez. Photoelectric artefact from optogenetics and imaging on microelectrodes and bioelectronics: New Challenges and Opportunities. *Journal of materials chemistry. B*, 3(25):4965–4978, jul 2015.

[92] Sanja Mikulovic, Stefano Pupe, Helton Maia Peixoto, George C Do Nascimento, Klas Kullander, Adriano B L Tort, and Richardson N Leão. On the photovoltaic effect in local field potential recordings. *Neurophotonics*, 3(1):15002, jan 2016.

[93] A. Kaar, S.J. Morley, and M.G. Rae. An efficient and cost-effective method of generating postnatal (p2âĂŞ5) mouse primary hippocampal neuronal cultures. *Journal of Neuroscience Methods*, 286:69 – 77, 2017.

[94] JE Huettner and RW Baughman. Primary culture of identified neurons from the visual cortex of postnatal rats. *Journal of Neuroscience*, 6(10):3044–3060, 1986.

[95] Alison Easter, M. Elizabeth Bell, James R. Damewood, William S. Redfern, Jean Pierre Valentin, Matthew J. Winter, Carlos Fonck, and Russell A. Bialecki. Approaches to seizure risk assessment in preclinical drug discovery. *Drug Discovery Today*, 14(17-18):876–884, 2009.

[96] Carlos Fonck, Alison Easter, Mark R. Pietras, and Russell A. Bialecki. *CNS Adverse Effects: From Functional Observation Battery/Irwin Tests to Electrophysiology*, pages 83–113. Springer Berlin Heidelberg, Berlin, Heidelberg, 2015.

Appendix A

Specific of hardware components

A.1 DLP projector

As the projector used in this experiment is an evaluation module for easy use of DMD, any projector that can perform the similar function with DMD and the associated controller should be able to replace it. For this particular projector, DLP3000 DMD was used with DLPC300 as its controller (Fig. A.1, A.2)

Product Folder

Sample & Buy

Technical Documents

Tools & Software

Support & Community

TEXAS INSTRUMENTS

DLP3000

DLPS022B –JANUARY 2012 –REVISED MARCH 2015

DLP3000 DLP® 0.3 WVGA Series 220 DMD

1 Features

- 0.3-Inch (7.62 mm) Diagonal Micromirror Array
  - 608 × 684 Array of Aluminum, Micrometer-Sized Mirrors Offering up to WVGA Resolution (854 × 480) Wide Aspect Ratio Display
  - 7.6-µm Micromirror Pitch
  - ±12° Micromirror Tilt Angle (Relative to Flat State)
  - Side Illumination for Optimized Efficiency
  - 5-µs Micromirror Crossover Time
- Highly Efficient in Visible Light (420 to 700 nm):
  - Window Transmission 97%
  - Micromirror Reflectivity 88%
  - Array Diffraction Efficiency 86%
  - Array Fill Factor 92%
  - Polarization Independent
- Package Footprint of 16.6-mm × 7-mm × 4.6-mm
- Low Power Consumption at 200 mW (Typical)
- Dedicated DLPC300 Controller for Reliable Operation
- Supports High-Speed Pattern Rates of 4000 Hz (Binary) and 120 Hz (8-Bit)
- 15-Bit, Double Data Rate (DDR) Input Data Bus
- 60- to 80-MHz Input Data Clock Rate
- Integrated Micromirror Driver Circuitry
- Supports 0°C to 70°C
- Package Mates to PANASONIC AXT550224 Socket

2 Applications

- Machine Vision
- Industrial Inspection
- 3D Scanning Such as Dental Scanners
- 3D Optical Metrology
- Automated Fingerprint Identification
- Face Recognition
- Augmented Reality
- Embedded Display
- Interactive Display
- Information Overlay
- Spectroscopy
- Chemical Analyzers
- Medical Instruments
- Photo-Stimulation
- Virtual Gauges

3 Description

The DLP3000 digital micromirror device (DMD) is a digitally-controlled micro-opto-electromechanical system (MOEMS) spatial light modulator (SLM) optimized for small form-factor applications. When coupled to an appropriate optical system, the DLP3000 can be used to modulate the amplitude and direction of incoming light. The DLP3000 creates highly flexible light patterns with speed, precision, and efficiency.

Architecturally, the DLP3000 is a latchable, electrical-in/optical-out semiconductor device. This architecture makes the DLP3000 well-suited for use in applications such as 3D scanning or metrology with structured light, augmented reality, microscopy, medical instruments, and spectroscopy. The compact physical size of the DLP3000 is well-suited for portable equipment where small form factor and lower cost are important. The compact package complements the small size of LEDs to enable highly-efficient, robust light engines.

The DLP3000 is one of two devices in the DLP® 0.3 WVGA chipset. Proper function and reliable operation of the DLP3000 requires that it be used in conjunction with the DLPC300 controller. See the DLP 0.3 WVGA chipset data sheet (DLPZ005) for further details.

Device Information[1]

PART NUMBER	PACKAGE	BODY SIZE (NOM)
DLP3000	LCCC (50)	16.6 mm × 7.0 mm × 4.6 mm

(1) For all available packages, see the orderable addendum at the end of the data sheet.

Simplified Diagram
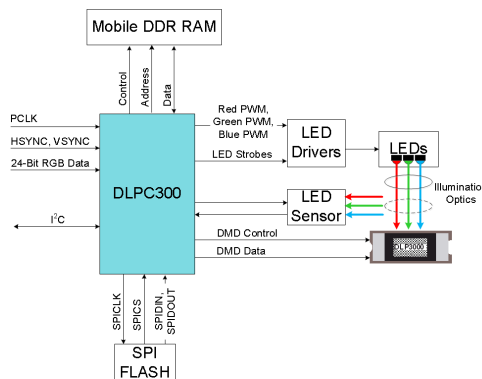
Figure A.1: Specification sheet for DLP3000 DMD.

Product Folder

Sample & Buy

Technical Documents

Tools & Software

Support & Community

Reference Design

TEXAS INSTRUMENTS

DLPC300

DLPS023C – JANUARY 2012 – REVISED AUGUST 2015

DLPC300 DLP® Digital Controller for the DLP3000 DMD

1 Features

- Required for Reliable Operation of the DLP3000 DMD
- Multi-Mode, 24-Bit Input Port:
  - Supports Parallel RGB With Pixel Clock Up to 33.5 MHz and 3 Input Color Bit-Depth Options:
    - 24-Bit RGB888 or 4:4:4 YCrCb888
    - 18-Bit RGB666 or 4:4:4 YCrCb666
    - 16-Bit RGB565 or 4:2:2 YCrCb565
  - Supports 8-Bit BT.656 Bus Mode With Pixel Clock Up to 33.5 MHz
- Supports Input Resolutions 608 × 684, 864 × 480, 854 × 480 (WVGA), 640 × 480 (VGA), 320 × 240 (QVGA)
- Pattern Input Mode
  - One-to-One Mapping of Input Data to Micromirrors
  - 1-Bit Binary Pattern Rates up to 4000-Hz
  - 8-Bit Grayscale Pattern Rates up to 120-Hz
- Video Input Mode with Pixel Data Processing
  - Supports 1- to 60-Hz Frame Rates
  - Programmable Degamma
  - Spatial-Temporal Multiplexing (Dithering)
  - Automatic Gain Control
  - Color Space Conversion
- Output Trigger Signal for Synchronizing With Camera, Sensor, or Other Peripherals
- System Control:
  - I²C Control of Device Configuration
  - Programmable Current Control of up to 3 LEDs
  - Integrated DMD Reset Driver Control
  - DMD Horizontal and Vertical Display Image Flip
- Low-Power Consumption: Less than 93 mW (Typical)
- External Memory Support:
  - 166-MHz Mobile DDR SDRAM
  - 33.3-MHz Serial FLASH
- 176-Pin, 7 × 7 mm With 0.4-mm Pitch NFBGA Package

2 Applications

- 3D Metrology
- 3D Scanning
- Factory Automation
- Fingerprint Identification
- Fringe Projection
- Industrial In line Inspection
- Robotic Vision
- Stereoscopic Vision
- Chemical Sensing
- Mobile Sensing
- Spectroscopy
- Augmented Reality
- Information Overlay
- Medical Instruments
- Virtual Gauges

3 Description

The DLPC300 controller provides a convenient, multifunctional interface between user electronics and the DMD, enabling high-speed pattern rates (up to 4-kHz binary), providing LED control, and data formatting for multiple input resolutions. The DLPC300 digital controller, part of the DLP3000 chipset, is required for reliable operation of the DLP3000 DMD. The DLPC300 also outputs a trigger signal for synchronizing displayed patterns with a camera, sensor, or other peripherals.

Device Information[1]

PART NUMBER	PACKAGE	BODY SIZE (NOM)
DLPC300	NFBGA (176)	7.00 mm × 7.00 mm

(1) For all available packages, see the orderable addendum at the end of the data sheet.

Typical Embedded System Block Diagram
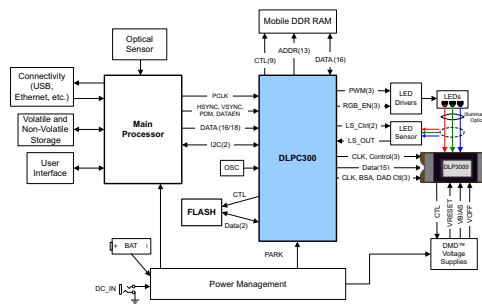
An IMPORTANT NOTICE at the end of this data sheet addresses availability, warranty, changes, use in safety-critical applications, intellectual property matters and other important disclaimers. PRODUCTION DATA.

Figure A.2: Specification sheet for DLPC300 DLP Digital Controller.

A.2   Optic systems

Doublet lenses	L_1	L_2
Item number	AC254-035-A-ML	AC508-200-A-ML[d]
Lens Diameter(mm)	25.4	50.8
f^a(mm)	35	200
f_b^a(mm)	27.3	193.7
WD^c (mm)	24.3	190.7
R_1^a (mm)	24	109.86
R_2^a (mm)	-19.1	-93.11
R_3^a (mm)	-102.1	-376.3
t_{c1} (mm)	12	8.5
t_{c2} (mm)	2	2
t_e (mm)	9.6	6.7
Materials	N-BAF10/N-SF6HT	N-BK7/SF2

Table A.1: Specification of the doublet lenses used on the optical system
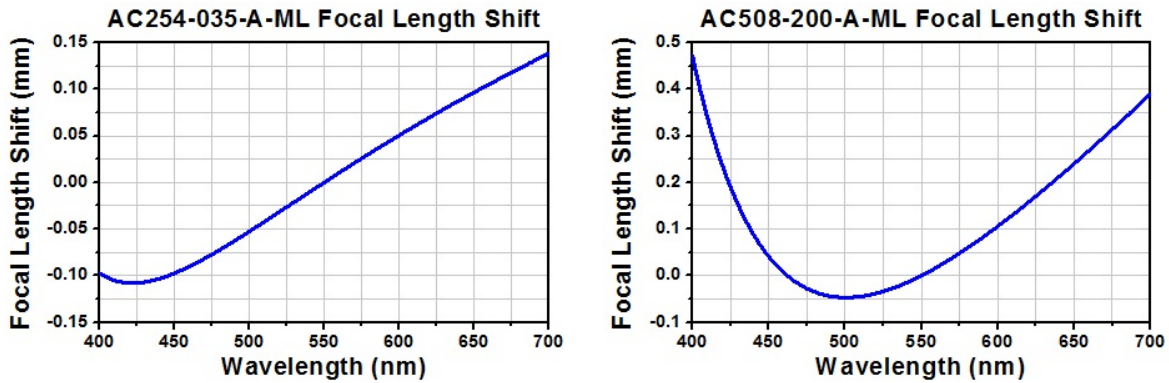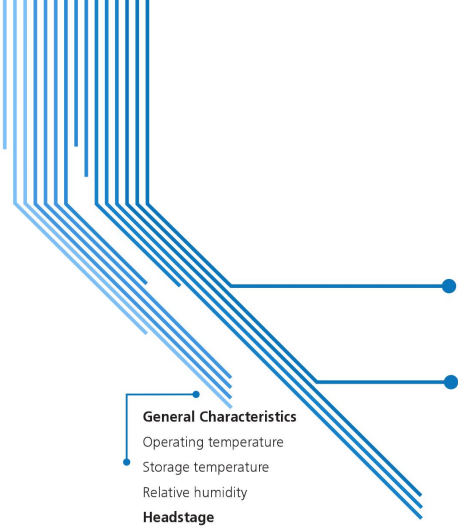
Figure A.3: Focal length shift according to the light wavelength.

Objective lens	
Model number	MLWD-5X
Objective Type	Long Working Distance
Magnification	5x
Numerical Aperture	0.14
Wavelength Range	400-700 nm
Effective Focal Length (EFL)	40 mm
Working Distance	34 mm
Design Tube Lens Focal Length	200 mm
Thread Type	M26 x 36 TPI
Parfocal Length	95 mm

Table A.2: Specification of long working distance objective lens

A.3 Data acquisition devices

MEA2100-System

Technical Specifications

General Characteristics

Operating temperature	10 °C to 50 °C
Storage temperature	0 °C to 50 °C
Relative humidity	10 % to 85 % , non-condensing

Headstage

Dimensions (W x D x H)	250 mm x 151 mm x 25 mm
Weight	± 1200 g
Type of headstage	MEA2100-HS32 for 32-electrode MEAs
	MEA2100-HS2x32 for two 32-electrode MEAs
	MEA2100-HS60 for 60-electrode MEAs
	MEA2100-HS2x60 for two 60-electrode MEAs
	MEA2100-HS120 for 120-electrode MEAs
	MEA2100-HS256 for 256-electrode MEAs

Integrated Amplifier

Number of analog recording channels	32, 60,120 or 252, depending on the type of the headstage
Data resolution	24 bit (16 bit, if operated with MC_Rack)
Signal input voltage range	MC_Rack: from ± 4.9 mV to ± 500 mV
	Multi Channel Experimenter: ± 500 mV
	± 250 mV with MEA2100-HS256
Bandwidth	DC to 10 kHz, software controlled
Sampling frequency per channel	up to 50 kHz, software controlled
Input impedance	1 GΩ || 10 pF

Intergated Stimulus Generator

Output current	± 1.5 mA @ ± 16 V complicance voltage
Output voltage	± 10 V @ ± 20 mA max. compliance current
Stimulation pattern	MC_Rack: rectangle (biphasic, monophasic, pulse trains)
	Multi Channel Experimenter: almost arbitrary patterns
Number of stimulation channels	3 independent stimulation patterns per 60 channels
	2 independent stimulation patterns with MEA2100-HS256
Resolution	16 bit
Time resolution	20 µs

Integrated Heating Element

Temperature sensor type	Pt 100 (with four wire connection, compatible with TCX)
Accuracy	± 0.1 °C

Interface Board „MCS-IFB 3.0 Multiboot" and Connectors

Dimensions (W x D x H)	250 mm x 83 mm x 25 mm
Weight	300 g

Front Panel

4 Digial inputs	Lemo connector, EPL 00250 NTN
4 Digital outputs	Lemo connector, EPL 00250 NTN
2 Auxiliary channels (not in use)	Lemo connector, EPL 00250 NTN

March 2019

Figure A.4: Specification sheet for MEA-2100 system.

MEA2100-System

Technical Specifications

Rear Panel

1 16 Bit Digital In / Out	68-pin MCS standard connector
1 8-Channel Analog In	10-pin connector (2.54 mm grid), dual row standard IDC
2 Analog Inputs	Lemo connector, EPL 00250 NTN
Signal input range for analog channels	± 2500 mV
Gain for analog channels	2 *
1 Digital signal processor DSP port	20-pin JTAG connector (1.27 / 2.54 mm grid), dual row
2 USB 3.0 ports	USB 3.0 super speed cable (type A - micro B)
Power supply	MPU 30, PWR DC 0.85 x 2.75 mm
Ground	Common jack 4 mm, banana plug
1 Audio output	Stereo jack 3.5 mm

Side Panel

2 Interface board to headstage connectors	External power over serial ATA (eSATAp)

Power Supply Unit (MPU 30)

Input voltage	90 - 264 VAC @ 47 - 63 Hz
Output voltage	11 - 13 V
Max. power	30 W
Mark of conformity	CE, TÜV, cUL
European standard	EN60601

Software

Operatring system Microsoft Windows ®	Windows 10, 8.1, and Windows 7 (32 or 64 bit), English and German version supported
Data acquisition and analysis software	
Multi Channel Experimenter	Version 1.5.1 and higher
Multi Channel Analyzer	Version 1.5.1 and higher
MC_Rack	Version 4.1.1 and higher
Data export software	
Multi Channel DataManager	Version 1.6.1 and higher, HDF5 (Madlab, Python, NEX (NeuroExplorer), CED (Spike), ASCII
MC_DataTool	Version 2.6.3 and higher Axion binary file, ASCII, binary file

* Important: In MC_Rack software the scaling of the analog channels is not correct for a factor of 2, because the gain of the analog channels is not considered.

API
Advanced Photonix, Inc.

PACKAGE DIMENSIONS INCH [mm]

.200 [5.08]
.080 [2.03]

BNC CONNECTOR ANODE

Ø.695 [17.65]
95° VIEWING ANGLE

Ø.975 [24.67]

BNC CONNECTOR CATHODE

±.010 [0.25]
1.070 [27.18]

CHIP DIMENSIONS INCH [mm]

.479 [12.17] SQUARE
Ø.444 [11.28] ACTIVE AREA

BNC PACKAGE
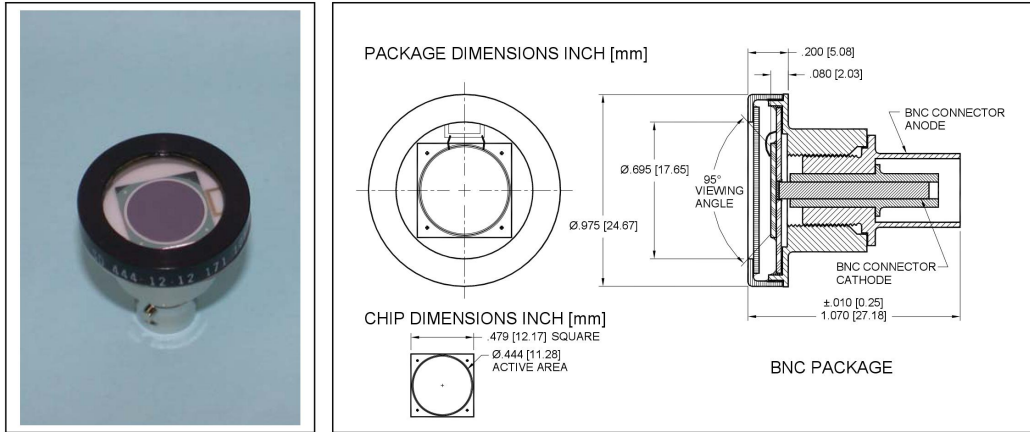
FEATURES
• Low noise
• Blue enhanced
• High shunt resistance
• High response

DESCRIPTION
The **SD 444-12-12-171** is a blue enhanced silicon PIN photodiode, packaged in a hermetic BNC connector package.

APPLICATIONS
• Instrumentation
• Industrial
• Medical

ABSOLUTE MAXIMUM RATING (TA)= 23°C UNLESS OTHERWISE NOTED

SYMBOL	PARAMETER	MIN	MAX	UNITS
V_{BR}	Reverse Voltage		75	V
T_{STG}	Storage Temperature	-55	+150	°C
T_O	Operating Temperature	-40	+125	°C
T_S	Soldering Temperature*		+240	°C

* 1/16 inch from case for 3 seconds max.

SPECTRAL RESPONSE
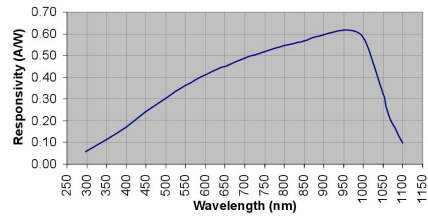
ELECTRO-OPTICAL CHARACTERISTICS RATING (TA)= 23°C UNLESS OTHERWISE NOTED

SYMBOL	CHARACTERISTIC	TEST CONDITIONS	MIN	TYP	MAX	UNITS
I_D	Dark Current	V_R = 5V		13.0	52.0	nA
R_{SH}	Shunt Resistance	V_R = 10 mV	35			MΩ
C_J	Junction Capacitance	V_R = 0 V, f = 1 MHz		725		pF
		V_R = 5 V, f = 1 MHz		213		
λ range	Spectral Application Range	Spot Scan	350		1100	nm
R	Responsivity	λ = 450 nm V, V_R = 0 V	0.20	0.28		A/W
V_{BR}	Breakdown Voltage	I = 10 μA		50		V
NEP	Noise Equivalent Power	V_R = 0V @ λ = Peak		1.2×10^{-13}		W/$\sqrt{Hz}$
t_r	Response Time**	RL = 50 Ω, V_R = 0 V		190		nS
		RL = 50 Ω, V_R = 10 V		13		

**Response time of 10% to 90% is specified at 660nm wavelength light.

Information in this technical datasheet is believed to be correct and reliable. However, no responsibility is assumed for possible inaccuracies or omission. Specifications are subject to change without notice.

Advanced Photonix Inc. 1240 Avenida Acaso, Camarillo CA 93012 • Phone (805) 987-0146 • Fax (805) 484-9935 • www.advancedphotonix.com

Figure A.5: Specification sheet for the photodiode.

64

Appendix B

Software used in the research

B.1 Creating patterns.

Python code used for the light pattern production is shown below. The code was created by Chris Park and modified by Seohyun Shim. It takes multiple arguments with the first being the name of the produced image and the following arguments are the electrodes that are lit up.

Listing B.1: Raw code for pattern generation

```python
import numpy as np
import scipy.misc as smp
import sys




#order is (y,x) instead of (x,y)
# A dictionary containing all the electrode positions were determined
# All the coordinates are the upper right corner of the rectangle
```

```
test = {
    #first row (d1-j1)
    "d1":[[31,233]],
    "e1":[[31,261]],
    "f1":[[31,289]],
    "g1":[[31,317]],
    "h1":[[31,345]],
    "j1":[[31,373]],
    #second row (c2-k2)
    "c2":[[87,205]],
    "d2":[[87,233]],
    "e2":[[87,261]],
    "f2":[[87,289]],
    "g2":[[87,317]],
    "h2":[[87,345]],
    "j2":[[87,373]],
    "k2":[[87,401]],
    #third row (b3-l3)
    "b3":[[143,177]],
    "c3":[[143,205]],
    "d3":[[143,233]],
    "e3":[[143,261]],
    "f3":[[143,289]],
    "g3":[[143,317]],
    "h3":[[143,345]],
    "j3":[[143,373]],
    "k3":[[143,401]],
    "l3":[[143,429]],
    #fourth row (a4-m4)
    "a4":[[199,149]],
    "b4":[[199,177]],
    "c4":[[199,205]],
    "d4":[[199,233]],
```

```
"e4":[[199,261]],
"f4":[[199,289]],
"g4":[[199,317]],
"h4":[[199,345]],
"j4":[[199,373]],
"k4":[[199,401]],
"l4":[[199,429]],
"m4":[[199,457]],
#fifth  row  (a5-m5)
"a5":[[255,149]],
"b5":[[255,177]],
"c5":[[255,205]],
"d5":[[255,233]],
"e5":[[255,261]],
"f5":[[255,289]],
"g5":[[255,317]],
"h5":[[255,345]],
"j5":[[255,373]],
"k5":[[255,401]],
"l5":[[255,429]],
"m5":[[255,457]],
#sixth  row  (a6-m6)
"a6":[[311,149]],
"b6":[[311,177]],
"c6":[[311,205]],
"d6":[[311,233]],
"e6":[[311,261]],
"f6":[[311,289]],
"g6":[[311,317]],
"h6":[[311,345]],
"j6":[[311,373]],
"k6":[[311,401]],
"l6":[[311,429]],
```

```
"m6":[[311,457]],
#seventh row (a7-m7)
"a7":[[367,149]],
"b7":[[367,177]],
"c7":[[367,205]],
"d7":[[367,233]],
"e7":[[367,261]],
"f7":[[367,289]],
"g7":[[367,317]],
"h7":[[367,345]],
"j7":[[367,373]],
"k7":[[367,401]],
"l7":[[367,429]],
"m7":[[367,457]],
#eigth row (a8-m8)
"a8":[[423,149]],
"b8":[[423,177]],
"c8":[[423,205]],
"d8":[[423,233]],
"e8":[[423,261]],
"f8":[[423,289]],
"g8":[[423,317]],
"h8":[[423,345]],
"j8":[[423,373]],
"k8":[[423,401]],
"l8":[[423,429]],
"m8":[[423,457]],
#ninth row (a9-m9)
"a9":[[479,149]],
"b9":[[479,177]],
"c9":[[479,205]],
"d9":[[479,233]],
"e9":[[479,261]],
```

```
"f9":[[479,289]],
"g9":[[479,317]],
"h9":[[479,345]],
"j9":[[479,373]],
"k9":[[479,401]],
"l9":[[479,429]],
"m9":[[479,457]],
#tenth row (b10-l10)
"b10":[[535,177]],
"c10":[[535,205]],
"d10":[[535,233]],
"e10":[[535,261]],
"f10":[[535,289]],
"g10":[[535,317]],
"h10":[[535,345]],
"j10":[[535,373]],
"k10":[[535,401]],
"l10":[[535,429]],
#eleventh row (c11-k11)
"c11":[[591,205]],
"d11":[[591,233]],
"e11":[[591,261]],
"f11":[[591,289]],
"g11":[[591,317]],
"h11":[[591,345]],
"j11":[[591,373]],
"k11":[[591,401]],
#twelvth row (d12-j12)
"d12":[[647,233]],
"e12":[[647,261]],
"f12":[[647,289]],
"g12":[[647,317]],
"h12":[[647,345]],
```

```python
    "j12":[[647,373]]
    }


data = np.zeros( (684,608,3), dtype=np.uint8 )


# function for making a rectangle for covering the electrode
def make_electrode(data,y,x,y_length=8,x_length=4):
    new_y=list(range(y,y+y_length))
    new_x=list(range(x,x+x_length))
    for i in new_y:
        for j in new_x:
            data[i,j]=[255,255,255]
    return 0



for x in sys.argv[2::]:
    for y in test[x]:
        make_electrode(data,y[0],y[1])
        #data[y[0]][y[1]]=[255,255,255]

#img = smp.toimage( data )
from PIL import Image
img = Image.fromarray( data )
img.save(sys.argv[1]+".bmp")
```

B.2   Pattern projection

An example of using the DLP projector GUI is shown in Fig. B.1. The pattern used on this GUI is generated using MBMC parser with the file provided by Texas Instrument. An image list containing the names of the images that are projected as patterns is needed. By using the bin and readme files for determining the sequence and the image list file that dictates which images are projected at what order, a repeating pattern is produced from the DLP projector. However, TI is no longer providing the service for the patterns. Therefore, MBMC pattern mode can only be used for device validation.
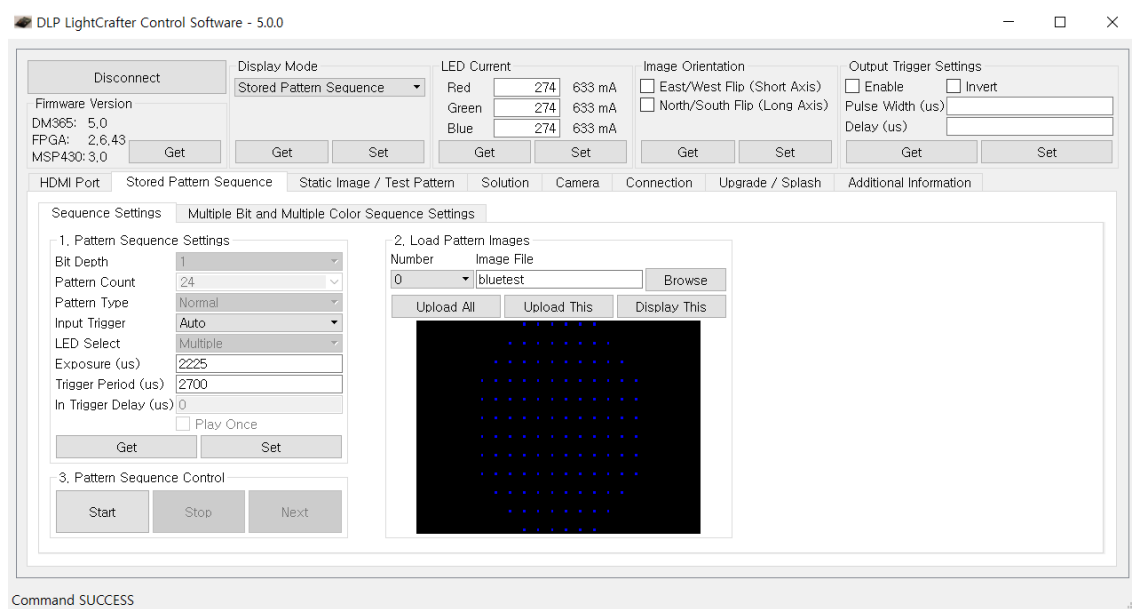
Figure B.1: DLP projector GUI using MBMC mode.

************WARNING************>>>>>>>>>>>>>>>>>>THIS IS AUTO GENERATED FILE DO NOT EDIT<<<<<<<<<<<<<<<<<

```
#===============================================================================
=======================
#   Multiple Bit Depth and Multiple Color Pattern Sequence use instructions for DLP LightCrafter EVM
#----------------------------------------------------------------------------------------------------
#  Created on        : Monday, November 21, 2016 10:15:36 AM
#  Created by        : DLP LightCrafter Sequence Builder
#  Tool Version#     : 1.3.2
#  Pattern Seq Mode# : INTERNAL PRE-STORED PATTERNS
#  Exposure time     : 2225 uSec
#  Trig Period       : >= 2700 uSec
#----------------------------------------------------------------------------------------------------
```

The instructions provided below can be used to configure LightCrafter to
support Mulitple Bit Depth and Multiple Color pattern sequence.

1. Sequence Equation: 1bppX1R_1bppX1G_1bppX22B_2225uSec

2. Enable Mulitple Bit Depth and Multiple Color Pattern Sequence using TCP command (0x0A 0x01) ==>
StartVector = 0, NumOfVectors = 25

3. The pattern order used in the sequence is provided in the Table-0.

```
   Table-0: Pattern Order Table
   -----------  -------------------------  ----------------
   PATTERN NO.  PATTERN BIT-DEPTH (in bpp)  PATTERN COLOR
   -----------  -------------------------  ----------------


   1   1   Red

   2   1   Green

   3   1   Blue

   4   1   Blue

   5   1   Blue

   6   1   Blue

   7   1   Blue

   8   1   Blue

   9   1   Blue
```

Figure B.2: An example of readme file for pattern generation.

Appendix C

Animal testing

C.1   Genetic strain information

The strain used for the experiment is Tg (Thy1-COP4/EYFP)9Gfng/J from Jax Laboratory. The modified mouse with this strain expresses Channelrhodopsin-2 and Yello Fluorescent Protein (ChR2-YFP) in the brain including hippocampus, thus can have the neurons be activated using blue light ($\sim$470nm) (Fig. C.1).

As it includes fluorescent protein, the same method for genotyping the strain with Green Fluorescent Protein (GFP) can be used (Fig. C.2).

The Jackson Laboratory

B6.Cg-Tg(Thy1-COP4/EYFP)9Gfng/J

Stock No: 007615 | **Thy1-ChR2-YFP**

AVAILABLE

Also Known As: Thy1-ChR2-YFP

Tg(Thy1-COP4/EYFP)9Gfng (or Thy1-ChR2-YFP) transgeni
mice may be useful in optogenetic studies for rapid contro
motor behavior by addition or removal of light, for *ex vivo*
in vivo studies of neural circuitry/connectivity following
illumination, and for fluorescent labeling of *Thy1*-express
cells throughout the brain (including cortex, hippocampus
thalamus, midbrain, brainstem, cerebellar mossy fibers a
retinal ganglion cells).

Donating Investigator

Guoping Feng, Massachusetts Institute of Technology

Figure C.1: Detail on the strain.

74

Genetic Overview

Genetic Background	Generation
	N6+N6F6 (2019-05-17 00:00:00)

MOUSE STRAIN DATASHEET - 007615

The Jackson Laboratory

Tg(Thy1-COP4/EYFP)9Gfng

Allele Type
Transgenic (Reporter)

Research Applications

Research Tools

Neurobiology Research

Base Price

Starting at:

$278.00 Domestic price for female

348.51 Domestic price for breeder pair

⊖Detailed Description

These Thy1-ChR2-YFP founder line 9 transgenic mice express the light-activated ion channel, Channelrhodopsin-2 (from t green alga *Chlamydomonas reinhardtii*), fused to Yellow Fluorescent Protein (ChR2-YFP) under the control of the mouse thymus cell antigen 1 (*Thy1*) promoter. Hemizygotes are viable, fertile, normal in size and do not display any gross physic behavioral abnormalities. Expression of the transgenic ChR2-YFP fusion protein is detected throughout the brain, includin the cortex, hippocampus, thalamus, midbrain, brainstem, cerebellar mossy fibers and retinal ganglion cells. Neurons expressing the transgene are morphologically and physiologically comparable to non-mutant neurons. This mutant mous strain may be useful for *ex vivo* and *in vivo* neural circuitry mapping studies using light stimulation.

The ChR2-YFP fusion protein is composed of a *Chlamydomonas reinhardtii*-derived channelrhodopsin-2 (ChR2) fused in-f with an enhanced yellow fluorescent protein (EYFP).
The bacterial opsins are retinal-binding proteins that combine a light-sensitive domain with an ion channel or pump; prov light-dependent ion transport, membrane potential alteration, and sensory functions to bacteria. ChR2 functions as a blue driven cation channel that depolarizes the cell and causes action potentials. As such, illuminating ChR2-expressing neuro with blue light (~470 nm) leads to rapid and reversible photostimulation of action potential firing/neural activity in these c

This optogenetic strain is one of many from the same transgene creator/donating investigator with light-inducible neurob applications; including
Thy1-ChR2-YFP line 18 (Stock No. 007612),
Thy1-eNpHR-YFP line 2 (Stock No. 012332),
Thy1-eNpHR-YFP line 4 (Stock No. 012334),
Thy1-vChR1-YFP line 1 (Stock No. 012341),
Thy1-vChR1-YFP line 4 (Stock No. 012344),

Thy1-vChR1-YFP line 8 (Stock No. 012348),
Thy1-mhChR2-YFP Line 20 (Stock No. 012350),
Prv-mhChR2-YFP Line 15 (Stock No. 012355),
ChAT-ChR2-YFP line 5 (Stock No. 014545),
ChAT-ChR2-YFP line 6 (Stock No. 014546),
VGAT-ChR2-YFP line 8 (Stock No. 014548),
and TpH2-ChR2-YFP line 5 (Stock No. 014555).

MOUSE STRAIN DATASHEET - 007615

The Jackson Laboratory

View YFP fluorescence in sagittal brain sections for this strain.

Development

A transgenic construct containing Channelrhodopsin-2 from the green alga *Chlamydomonas reinhardtii* and Yellow Fluore
Protein fusion gene under the control of the mouse thymus cell antigen 1 promoter was injected into C57BL/6 X SJL F1 hy
donor eggs. Founder line 9 was subsequently established. The mice were backcrossed to C57BL/6 for six generations bef
arriving at The Jackson Laboratory.

Expression Data

Expressed Gene	*YFP*, Yellow Fluorescent Protein, jellyfish
Expressed Gene	*COP4*, Channelrhodopsin, Chlamydomonas
Site of Expression	widespread expression in the brain including the cortex, hippocampus, thalamus, midbrain, brainstem, cerebellar mossy fibers amd retinal ganglion cells; channelrhodopsin-2 and *YFP*

Control Suggestions

Noncarrier
000664 C57BL/6J
Additional Information
—

Selected References

Arenkiel BR; Peca J; Davison IG; Feliciano C; Deisseroth K;
Augustine GJ; Ehlers MD; Feng G. 2007. In vivo light-induced
activation of neural circuitry in transgenic mice expressing
channelrhodopsin-2. Neuron 54(2):205-18   PubMed:
17442243   MGI: J:122790

Tg(Thy1-COP4/EYFP)9Gfng

Allele Symbol: Tg(Thy1-COP4/EYFP)9Gfng   MGI↗

Allele Name	transgene insertion 9, Guoping Feng
Allele Type	Transgenic (Reporter)
Allele Synonym(s)	Tg(Thy1-COP4/EYFP)9Gfng; transgene insertion 9, Guoping Feng
Gene Symbol and Name	Tg(Thy1-COP4/EYFP)9Gfng MGI↗ , transgene insertion 9, Guoping Feng
Gene Synonym(s)	ChR2-YFP; Thy1-ChR2-YFP

Promoter	*Thy1*, thymus cell antigen 1, theta, mouse, laboratory
Expressed Gene	*YFP*, Yellow Fluorescent Protein, jellyfish
Expressed Gene	*COP4*, Channelrhodopsin, Chlamydomonas
Site of Expression	widespread expression in the brain including the cortex, hippocampus, thalamus, midbrain, brainstem, cerebellar mossy fibers amd retinal ganglion cells; channelrhodopsin-2 and *YFP*
Strain of Origin	C57BL/6 x SJL
Chromosome	UN
General Note	Lines initiated from 7 of 10 transgenic founder mice exhibited expression of the chimeric protein in the central and/or peripheral nervous system, the specific pattern of expression varying among lines.
Molecular Note	This transgene gives rise to a fusion protein composed of the first 315 amino acids of the light-activated, non-specific ion channel chlamyopsin 4 (COP4), also known as channelopsin 2 (CHOP2) and as channelrhodopsin 2 (ChR2), from the green alga *Chlamydomonas reinhardtii* joined to enhanced yellow fluorescent protein. The chimeric cDNA has replaced the Thy1 coding sequence and its associated introns, which contain sequences directing expression in non-neuronal cell types. The vector contains the entire Thy1 gene (including the essential promoter and neuron-specific upstream regulatory sequences, 3' polyA signal sequences and neuronal-specific expression signal containing introns) with the coding region removed (from the ATG in exon to the end in exon 4, including intervening introns 2 and 3). Immunohistochemical analysis shows that mice with this transgene express the chimeric protein in neurons of several brain regions, including various nuclei of the brainstem, midbrain and thalamus; CA1 and CA3 pyramidal neurons of the hippocampus; strongly in layer 5 neurons of the cortex; and in retinal ganglion cells.

MOUSE STRAIN DATASHEET - 007615

The Jackson Laboratory

Disease Terms

Research Areas By Genotype

This mouse can be used to support research in many areas including:

- Research Tools
  - Neurobiology Research
    - cell marker
  - Fluorescent Proteins
  - Neurobiology Research
    - Fluorescent protein expression in neural tissue
    - Optogenetic and Chemogenetic tools
      - Channelrhodopsin expressing strains

Mammalian Phenotype Terms by Genotype

The following phenotype information is associated with a similar, but not exact match to this JAX® Mice strain

Genotype: Tg(Thy1-COP4/EYFP)9Gfng/0
        involves: C57BL/6 * SJL

normal phenotype
- no abnormal phenotype detected
  - *Normal* - neurons expressing EYFP show no signs of degeneration or altered morphology (MGI Ref ID J:122790)

Return to Protocol Search

Stock Number: **007615**

Strain Name: **B6.Cg-Tg(Thy1-COP4/EYFP)9Gfng/J**

Allele: Generic GFP

Protocol Name: Fluorescent Proteins (Generic GFP)

Method: Standard PCR

Version: 4.2

Created: 19-May -2017   Updated: 19-May -2017

Notes: This assay will NOT distinguish hemizygous from homozygous transgenic animals.

Expected Results: Transgene = 173 bp
                     Internal positive control = 324 bp

Gel Image

Image	Image file
	View
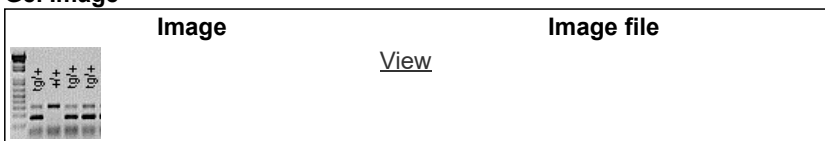
Separated by gel electrophoresis on a 1.5% agarose gel.

Protocol Primers

Primer	5' Label	Sequence 5' --> 3'	3' Label	Primer Type	Note
oIMR0872		AAG TTC ATC TGC ACC ACC G		Transgene	Reaction A GFP
oIMR1416		TCC TTG AAG AAG ATG GTG CG		Transgene	Reaction A GFP
oIMR7338		CTA GGC CAC AGA ATT GAA AGA TCT		Internal Positive Control Forward	Reaction A
oIMR7339		GTA GGT GGA AAT TCT AGC ATC ATC C		Internal Positive Control Reverse	Reaction A

Reaction   A

Reaction Component	Final Concentration	Unit
ddH2O	up to final volume	
Kapa 2G HS buffer	1.3	X
MgCl2	2.6	mM
dNTP KAPA	.26	mM
oIMR0872	.5	uM
oIMR1416	.5	uM
oIMR7338	.5	uM
oIMR7339	.5	uM
Glycerol	6.5	%
Dye	1	X
Kapa 2G HS taq polymerase	.03	U/ul
DNA	50-200	ng

Cycling

Step #	Temp °C	Time	Note
1	94	2 min	
2	94	20sec	
3	65	15sec	-0.5 C per cycle decrease
4	68	10sec	
5			repeat steps 2-4 for 10 cycles (Touchdown)
6	94	15sec	
7	60	15sec	
8	72	10sec	
9			repeat steps 6-8 for 28 cycles
10	72	2 min	
11	10		hold

Figure C.2: Genotyping method provided by the manufacturer.

C.2 IACUC protocol

The approved IACUC protocol for the animal testing necessary for the experiment is shown below. The protocol lasts for 3 years and includes plan for future multi-compartment electrode array experiment.

UCI Office of
Research
Research Management System

Animal Use Protocol (AUP-19-019)

Title

Tang Lab Mouse Protocol

General Information

AUP: AUP-19-019
Version: 29.0

Figure C.3: IACUC protocol.

Project Overview

Provide a non-technical, lay-language summary of your project.
Uncheck this box to remove all text from the box below

In our project, we are studying the network hierarchy of neuron activity. Although all neurons stimulate each other through action potential, some neurons are more likely to stimulate other neurons and less likely to take stimuli from others; we call this neurons "leader neurons." Because the leader neurons are more influential, we hypothesize that they play an essential role in communication between the hippocampal subregions of the brain that are involved in learning and memory; damage to leader neurons may be a contributing factor in neurodegenerative diseases such as schizophrenia and Alzheimer's.

We plan to study leader neurons in vitro where their features can be controlled more closely than in an in vivo model. We will harvest neurons from neonatal mice and study them in culture using multielectrode arrays (MEA) and digital light processing (DLP) projector, which will enable us to stimulate multiple neurons and study their propagation with high resolution.

Our research is novel in that we are incorporating LED light delivery to neurons cultured on a multielectrode array (MEA). Most in vitro neuron models use MEA, but most of the time they stimulate neurons using electrodes which introduce electrical artifacts. By using light to stimulate the neurons, we hope to enhance the resolution of the network activity propagation. Using a Digital Light Processing projector also allows us to stimulate many neurons simultaneously. This is useful because the network propagation in vivo is often not decided by a single neuron, but rather a small cluster of neurons. Therefore using a DLP projector along with MEA enables us to stimulate multiple neurons and study their propagation with high resolution.

Study Characteristics
Breeding
mouse(Thy1-ChR2-YFP), mouse(C57BL/6J)
> *You MUST create a separate Breeding study segment (describing breeding activities) in the Experimental Design Tab*
> *You MUST list Pain Category B animal numbers in the Animal Numbers Tab*

Project Continuation

Is this application a 3-year renewal of a previously approved protocol?
No - This is a new application

AUP: AUP-19-019
Version: 29.0

Funding Source	Funding Status	Award/Proposal #	Billing Account #
UROP	Awarded	90702s1	GF11700
NIH grant	Pending		

Funding & Billing Information

Other Funding Sources (not captured in table above)

Has the project undergone peer-review by an extramural sponsor/funding agency (e.g., NIH study section)?
No

PI Home Department
Uncheck this box to remove all text from the box below

Biomedical Engineering Department

Species

Mouse - Mus

Mouse - Mus

AUP: AUP-19-019
Version: 29.0

Species Justification

Provide scientific justification for why the proposed species is the most appropriate model for this research.
Uncheck this box to remove all text from the box below

There are several reasons for using a mouse for this research. The biggest reason is that research done on mice is known to be comparable to those that were found using human tissue. Therefore, we expect to be able to derive a conclusion from mice that apply to human's neuron network activity.

Also, genetic strain for the optogenetically modified mouse has been well established and is easy to obtain. This, along with the fact that culture preparation of these tissues are very well defined and can be generated and examined quickly and easily allows us to reduce the number of animals needed for the experiment. Housing and maintenance of the animals are relatively easy as well.

For our particular experiment, we will be using Thy1-ChR2-YFP line mouse. This line of mouse is known to have a wide expression in the brain including hippocampus which is where we need our Channelrhodopsin II to be.

Animal Characteristics

List the specific strains that will be used.
Uncheck this box to remove all text from the box below

Thy1-ChR2-YFP : has hippocampal neurons that are genetically modified to receive light as stimulus. experimental group.

C57BL/6J : wildtype. used for control

Phenotypic Abnormalities or Special Health Conditions
Uncheck this box to remove all text from the box below

Thy1-ChR2-YFP line mouse is genetically modified to have Channelrhodopsin and Yellow Fluorescent Protein gene expressed in the brain. This allows the neurons harvested from them to be visible under fluorescent imaging and take blue(480nm) light as stimuli.

Additional Information about Species/Strains

Rationale & Alternatives

Search Results

Date of Search	Time period from	Time period to	Database	# of Results	Keywords
Mar-08-2019	Jan-01-2000	Mar-08-2019	PubMed	23	hippocampus AND optogenetics AND electrode
Mar-08-2019	Jan-01-2000	Mar-08-2019	Web of Science	12	hippocampus AND optogenetics AND electrode

AUP: AUP-19-019
Version: 29.0

Database Searches

Discussion of Search Results
Uncheck this box to remove all text from the box below

Multielectrode array and optogenetics are commonly used for neuron study. However, they are not used in unison as much. We were able to find 12 other research on PubMed that uses optogenetics and multi-electrode array in studying network activity of hippocampal neurons. Most of the papers were on in vivo deep brain stimulation or using an electrophysiological method on brain slices. There was one paper called "Optogenetic stimulation effectively enhances intrinsically generated network synchrony" by El Hady et al. published in 2013, which applied blue light to cultured neurons on the multielectrode array. However, this study focuses on studying the overall activity of the cultured neuron depending on how the light frequency changes, therefore their method is not suitable for our purpose of identifying a certain group of neurons that are more influential than others in signal propagation.

Along with multielectrode array, using patch clamp with optogenetically modified neuron is another common way to study signal propagation of neurons. However due to their bulkiness, it is difficult to record from more than 4 to 12 neurons at a time. Because light stimulus has a much higher spatiotemporal resolution than electrical stimuli given by the electrode array, and because electrode from which we collect data has 120 acquisition sites compared to patch clamp, our device will be able to obtain

Other Sources Used to Consider Alternatives
Uncheck this box to remove all text from the box below

I have emailed Transgenic Mouse Facility on May 20th if they could help with getting the genetically modified mice we needed. However, they told me that they did not have the line we needed and their facility does not have the capacity to handle the additional breeding project.

Also in my own research, I could not find another lab that uses the same genetically modified mouse for in vitro research as they usually focused on certain disorder such as epilepsy or Alzheimer's, therefore introduce another modification in the mouse instead of having offsprings with only channelrhodopsin planted in the hippocampus.

AUP: AUP-19-019
Version: 29.0

Replacement

Discuss efforts to partially or fully replace live animals with in vitro models, (i.e. cell culture), computer simulation, or use of a less-sentient species (e.g. insects).
Uncheck this box to remove all text from the box below

Because we are building a device for cultured neurons to study the network activity in more controlled environment than in vitro, using a computer model to study the network activity is not applicable. For the 2D cultured system, another possible non-animal model would be to use induced pluripotent stem cell to generate neuronal tissue, but iPSC is not reliable when trying to obtain specific brain region.

No other cell lines are sufficiently similar to brain neurons or can replace the relevance of primary neurons from live animals for understanding and comparing the different network activity.

Reduction

Describe the steps you have taken to reduce the number of animals to the minimum required to obtain scientifically valid data.
Uncheck this box to remove all text from the box below

The use of primary neurons enables the multitudes of experiments under identical conditions to replace animal screening for figuring out network mechanisms. Thus far fewer animals and time will be needed.

Refinement

Explain how the experimental design and procedures have been refined to improve efficiency and minimize pain and distress.
Uncheck this box to remove all text from the box below

We have used Jove and PubMed database search to find out more about primary hippocampal neuron culture. Because we need postnatal mice, we will normally allow natural birth to obtain our sample. However, if euthanasia is needed for a dam, we will use CO2 to anesthetize the animal and decapitate afterward. Due to the effect it has on the neuronal development of the fetus, common anesthesia such as Isoflurane cannot be used on the dam.

we are also working with our collaborator who has refined acquiring electrical stimulation data from the MEA system for over 20 years to achieve maximum data collection from minimal use of animals. With his help, we will be recording a terabyte of neuronal activity from 120 electrodes in a few days of monitoring our in vitro networks

AUP: AUP-19-019
Version: 29.0

Study Segments

Experimental Design	Species
mouse study	Mouse - Mus
breeding colony	Mouse - Mus

mouse study

Species

 Mouse - Mus

Endpoints

Experimental Endpoints
Uncheck this box to remove all text from the box below

For the animals, their endpoints will be their age(P3-P5) at which time they will be anesthetized and decapitated.

Humane Endpoints

Animal Monitoring

Animal Monitoring Details

Clinical Signs or Symptoms of Pain/Distress

Management Plan for Animal Monitoring

Documentation of Animal Monitoring

Euthanasia

Will animals be euthanized at the end of the experiments?
Yes

> *Indicate the euthanasia methods that will be used on the animals from these experiments - Check all that apply*
> **Other**

No experiments will be performed with live animals; P3-P5 pups will be anesthetized via hypothermia and then decapitated. Brains will be harvested for in vitro experiments.

> *You MUST…*

Experimental Design Summary

> *Does this study segment tab describe the establishment and maintenance of a breeding colony?*
> **No - This study segment tab describes EXPERIMENTS (complete all questions below)**

> *Provide a concise description of the experimental design, describing all experiments to be performed.*
> **Uncheck this box to remove all text from the box below**

Neurons from genetically modified mouse brains are isolated from freshly euthanized mice in order to study the presence of leader neuron in the hippocampus using optogenetics and electrode array. The neurons will be extracted from different subregions of the hippocampus, specifically, the entorhinal cortex (EC), the dentate gyrus (DG), Cornu Ammonis 1 (CA1), and CA3. These neurons will be plated at a density of 1000 cells/mm2. Those from each of the 4 subregions will be plated in a separate chamber. At the start of the culture, we do not expect structured interconnectivity. At about 3 weeks post-culture, we expect the neurons to make connections. At this point, we will proceed with our experiments with measuring electrical activities, stimulating with electrical and optical spikes.

Understanding the leader neuron, which we believe to be the major factor in communication between subregions of the hippocampus, will give us fundamental knowledge of the network activity in the brain and provide insight into diseases that are caused by the disruption of neuron networks such as schizophrenia and Alzheimer. We chose this method of culturing neurons on top of the electrode array for this hypothesis because it is more controllable and has a higher spatiotemporal resolution than in vivo light stimulation. This can give us the result that is derived only from the light stimulus we provided to the neurons.

Leader neuron and follower neuron will be determined by observing the stimuli acquired

AUP: AUP-19-019
Version: 29.0

by electrode array via data post-processing. Leader neuron has a tendency to stimulate more neurons than standard neurons; i.e. it is more likely to result in more stimulation over the majority of the neuron compared to regular neuron.

The data will be recorded via electrode using a data acquisition device connected to a computer which allows us to see how much electrical signal each electrode are sensing when a neuron is stimulated. Therefore when light stimulates a neuron and initiates action potential, the electrode on which the neuron is cultured on top of will send that electrical data to the computer and allow us to see which electrode is getting stimulated.

We will perform one experiment to acquire data per month where 1 experimental group and 1 control group will be used. The experimental group will comprise of 4 cultures of genetically modified mouse tissues, and the control group will comprise of 4 cultures of wild-type tissues. Each culture will be derived from one pup. One litter gives us about 6-8 mice, half of which ideally will be genetically modified pups and the other half wild-type pups. These will serve as both the experimental and control pups. If the litter yields more than we need, we will keep the surplus as future breeder mice or use for additional experiments. The breeding will be performed once a month. The rest of the time will be dedicated to culturing neuron to build enough network (2-3 weeks) and post-processing the data we acquired.

Wild-type control is needed for this experiment to check for possible background noise, e.g. photovoltaic effect where light alone cause voltage in the electrode. Having the wildtype will help to adjust our light intensity to minimize that effect.

Four pups from each group will be used to harvest the tissue to form one culture from each pup. The culture can be maintained for up to 3 weeks. Producing and maintaining multiple samples is important to get a reliable result through repetition.

Pups will be anesthetized on the ice, decapitated and the brain removed for neuron culture. Subregions of the hippocampus are dissected, neurons isolated and placed in the compartment over an electrode array. Different configurations, cell densities, and stimulation protocols enable us to determine the nature of information transfer between the leader and follower neurons. Through this, we propose to identify the role of leader neuron in the communication between the subregions of the hippocampus.

Animal number calculation for experimental part mouse study

		Max	Description
	(	4	Experimental pups per experiment
+	4	)	control pups per experiment
*		12	number of culture per year
*		3	number of years for the protocol
		288	**Mouse - Mus**

Copy IACUC SOP templates

Procedure Descriptions

Euthanasia using CO2 Inhalation: Rodents will be placed in the euthanasia chamber and exposed to CO2 gas from a compressed gas canister via gradual fill method utilizing a displacement rate from 10% - 30% of the chamber volume. Where possible, animals will be euthanized in their home cage. All rodents euthanized with CO2 will undergo a secondary physical method of euthanasia to ensure death.

anesthesia via hypothermia: Mouse pups will be anesthetized by being placed on a paper towel on top of ice for 10-20 min. The anesthetized pups will be decapitated and then neuronal tissue will be harvested afterward.

Mouse - Mus

breeding colony

Species

Mouse - Mus

Endpoints

Experimental Endpoints

Humane Endpoints

AUP: AUP-19-019
Version: 29.0

Animal Monitoring

Animal Monitoring Details

Clinical Signs or Symptoms of Pain/Distress

Management Plan for Animal Monitoring

Documentation of Animal Monitoring

Euthanasia

Will animals be euthanized at the end of the experiments?

Experimental Design Summary

Does this study segment tab describe the establishment and maintenance of a breeding colony?
Yes - This study segment tab describes a Breeding Colony
Breeding Colony Justification
Uncheck this box to remove all text from the box below

Our research requires us to use mouse pup less than 5 days old, ideally P0-P1, due to the fact that neuron from adult mouse does not form networks with other neurons as easily. Because such young pups are not available via commercial means, we need to keep a breeding colony to obtain our sample.

Identification
Ear Notch
Genotyping
Tail Clip
    21 days old or less
Weaning Offspring
21 days or less
Will any drugs or agents be administered to breeding colony animals? (This includes special foods to enhance breeding performance)
No
Euthanasia of Breeding Colony Animals
Inhalant Overdose (CO2, Isoflurane, etc.) followed by secondary physical method
    Indicate the inhalant that will be used to overdose:
    CO2
    Isoflurane
    Secondary physical method:
    Cervical Dislocation
    Decapitation
You MUST...
SKIP QUESTIONS BELOW

Provide a concise description of the experimental design, describing all experiments to be performed.

Animal number calculation for experimental part breeding colony

Mouse - Mus		Max	Description
		10	Thy1-ChR2-YFP breeding pair
	*	3	number of years in protocol
		30	**Mouse - Mus**

Copy IACUC SOP templates

AUP: AUP-19-019
Version: 29.0

Procedure Descriptions

We will use the tail clip method to genotype the mice at P0 to P1 and apply permanent marker on the pup's body to identify them temporarily. After the pups had been genotyped, we will choose a breeder pair and euthanize the rest while harvesting neural tissue as needed when pups are around P3, P5 at the latest. The marker should be applied as frequently as necessary as it may come off in 3 - 4 days. When the mice are old enough (at least 10 days) the ear notch method will be used to identify them.

The breeder pair for genetically modified mice will be hemizygous x noncarrier(wildtype) as homozygous tend to have abnormalities that may affect the sample.

	Thy1-ChR2-YFP	0
0	Thy1-ChR2-YFP /0	0/0
0	Thy1-ChR2-YFP /0	0/0

Ideally, the ratio of hemizygous pups should be 50% and we should get at least 3-4 genetically modified pups and a similar number of wildtype pups.

After the first breeding, if the number of pups that has the allele is less than 2, we will perform another breeding immediately with another breeder pair. In other cases when we do get enough pups, 4 to 5 breeder pairs will take turns breeding so the same pair will normally breed every 3 months instead of every month.

The breeder pair will be replaced after the age of 7-8 months. They will be euthanized using CO_2 euthanasia followed by decapitation.

Euthanasia via CO_2 Inhalation: Rodents will be placed in the euthanasia chamber and exposed to CO_2 gas from a compressed gas canister via gradual fill method utilizing a displacement rate from 10% - 30% of the chamber volume. Where possible, animals will be euthanized in their home cage. All rodents euthanized with CO_2 will undergo a secondary physical method of euthanasia, i.e. decapitation to ensure death.

Mouse - Mus

Total number of animals

Species			Max
Mouse - Mus			318

USDA Pain Category	Species	Number of Animals	Number of Animals
USDA Category B	Mouse - Mus	30	0
USDA Category C	Mouse - Mus	288	0

Animal Numbers Justification

Explain how the animal numbers were determined.
Uncheck this box to remove all text from the box below

Given the number of experimental configurations, the number of factors examined with each, and the minimum number of repetitions (including 30% failures), up to 5 pairs of breeder mice will be necessary to prepare the appropriate numbers of hippocampal neuron cultures from 96 pups per year. Four pups, i.e. 4 transgenic pups and 4 wildtype pups will be needed per experiment to provide sufficient neurons for the experiments. The control pups are the wild-type siblings of the transgenic mice, offsprings of the same breeder pairs. They are reared under the same conditions as experimental transgenic mice. These experiments will be performed every month due to the time it takes for the neurons to grow and the data post-processing following the data acquisition. The 12 experiments per year is needed to provide stastically significant results.

We have 50% chance of getting either heterozygous or wildtype mice. Therefore, we expect to use 8 pups, 4 pups for experimental and 4 pups for control to harvest neurons from. Twice a year some mice will be reserved for replenishing the breeder stock. We need one heterozygous and one wildtype to produce our litter. Two heterozygous mice will not be crossed due to complications that occur in homozygous mice. Therefore, heterozygous and wildtype mouse will both be used. According to Dr. Brewer, ten breeders, five pairs in Category B is enough. Because each pair can breed every 2-3 months, a different pair will be used every month to produce the litter. As every breeder pair will be replaced after the mouse reach 8 months, we will get 3-4 litters from each pair.

Will animals experience unrelieved pain/distress (category E procedures)?
No

Drugs & Agents

Anesthesia

Will animals receive anesthesia agents?
Yes

Species *(receiving the drug/agent)*	Drug/Agent	Dose Range *(mg/kg body wt)*	Route *(SQ, IP, IV, IM, etc.)*	Frequency *(how often?)*	Duration *(how long?)*
mouse	ice, hypothermia for pups	to effect	surround	once	10-15min

How will the anesthesia be administered to the animals?

Will anesthetic GAS be used?
Yes

PLEASE DISREGARD - Anesthetic gases will not be used.

Analgesia

Will animals receive analgesics, sedatives, or other therapeutic agents (e.g. antibiotics, supplemental fluids, etc.)?
No

Experimental & Other Agents

Will animals receive experimental or any other agents (not captured in tables above)?
No

Will Controlled Substances be used?
No

Will non-pharmaceutical grade (i.e. chemical grade) agents be used in live animals?
No

Animal Locations & Husbandry

Food or Water Variations

Indicate the food or water variations that will be implemented in this protocol - Check all that apply:

Justification for the Food or Water Variations

AUP: AUP-19-019
Version: 29.0

Animal Husbandry Variations

Indicate the animal husbandry variations that will occur - Check all that apply:

Justification for the Animal Husbandry Variations

Researcher-Maintained Animals

Will LAB STAFF provide basic routine husbandry and care for the animals?
No

Will animals be held in the lab (outside of the vivarium) for more than 12 hours?
No

An Emergency Plan is REQUIRED for the following scenarios:

Other Husbandry/Housing Variations

Describe any other variations or special considerations (not already captured in the sections above).

Animal Locations

Indicate all locations where live animal procedures and/or housing will take place - Check all that apply:
ULAR Vivarium
Lab areas (outside of the ULAR vivarium) OR non-ULAR vivarium

Building	Room #	Location will be used for:		
		Non-surgical Procedures	Surgeries	Housing > 12 hrs
Natural Science II	3410	X		

Will any live animals (owned by UCI) be taken to offsite (non-UCI) locations for procedures?
No

Hazards & Safety

Chemical Hazards

Requirements for the Use of Potentially Hazardous Chemicals or Agents:

Biological Materials, Primary Cells or Cell Lines

Requirements for Use of Biological Materials:

Biological or Cell Line	Species of origin	Date of Pathogen Testing	IBC Protocol #	IBC Approval Date	Special Precautions

Infectious Agents

Requirements for the Use of Infectious Agents:

Recombinant DNA

Preparation & Use of rDNA

Radioactive Hazards

Radiation Use Authorization (RUA) #:

Removal of Radioactive Waste & Monitoring of Radioactivity

Creation of New Transgenic Animals

Are you creating a NEW strain of transgenic animal by crossbreeding 2 different strains?
No

Animal Biosafety Levels

Indicate the animal biosafety levels - Check all that apply:
ABSL-1

Other Hazards or Safety Considerations

Other Protocol Information

Provide any other information about this animal-use protocol (that is not captured in any other sections or tabs).

Personnel

Principal Investigator (PI)

Tang, William

Faculty Sponsor

AUP: AUP-19-019
Version: 29.0

Co-Investigator/Senior Researcher

Shim, Seohyun

Research Personnel

Brewer, Gregory
Lassers, Samuel Brandon
Mohseni, Niam
Pavlov, Alon
Smiggs, Ethan Shane

Other Research Personnel

Additional Personnel Information

Emergency Contact Information
Uncheck this box to remove all text from the box below

Name	Phone #	
	Daytime	After-hours *(mobile/cell preferred)*
Gregory Brewer	949 824 3762	949 824 3762

Add New User

Training Requirements

AUP: AUP-19-019
Version: 29.0

PI Qualifications

Description of PI Qualifications
Uncheck this box to remove all text from the box below

As a full-time Biomedical engineering department faculty, Dr. William Tang is eligible to be a PI for this research. Although he is not experienced in animal experiments he acknowledges that as a PI he has the ultimate responsibility to the experiment.

Training Plan for Study Team Members
Uncheck this box to remove all text from the box below

Team members who will be conducting the research will be trained by reviewing procedure described on JOVE and also get guidance from our collaborator Dr. Brewer who had worked with mouse and rat hippocampal neuron culture for over 20 years. Dr. Stacey Kang from ULAR has also agreed to give us guidance on starting our breeding colony. We will be going through training provided by ULAR on the procedure that we need such as anesthesia and euthanasia.

Links to Other Protocols

Other Regulatory Review Requirements

Indicate if other regulatory reviews are required for this protocol - Check all that apply:

If additional details need to be discussed regarding any of the links above, describe them below.

PI Certification

PI Certification

I hereby acknowledge and assure the following:
By clicking this checkbox, I certify that the above statements are understood and will be followed by all research team members.

AUP: AUP-19-019
Version: 29.0